IONOSONDE NETWORK ADVISORY GROUP (INAG)*

Ionospheric Station Information

Bulletin No. 62**

CONTENTS

*Under the auspices of Commission G, Working Group G 1 of the International Union of Radio Science (URSI)

**Prepared by Phil Wilkinson, Vice Chair INAG,
IPS Radio and Space Services,
P O Box 1386, Haymarket, NSW 1240, AUSTRALIA

Issued by IPS Radio and Space Services on behalf of INAG.

If you wish to be in the INAG mailing list to receive this Bulletin notify the INAG Chair, Ray Conkright,
WDC-A for STP,
NOAA, Boulder, Colorado 80303, USA.

1 AN OBITUARY: DR. HARVEY CUMMACK

Harvey Cummack, who died December 1 1996, was born March 3 1929 in Auckland. His family moved to Christchurch when Harvey was eleven where he attended Christchurch Boys' High and then studied mathematics, at what was then Canterbury College, to Master of Science level (1951). Subsequently, he devoted his scientific life to the terrestrial ionosphere, first in the Geophysical Observatory (PELGO) within DSIR, and on retirement in 1987 at the Physics and Astronomy Department of the University of Canterbury.

The importance of this region of the Earth's atmosphere, which is partially ionised by solar radiation, was recognised early this century as the agent for making long-distance high-frequency radio propagation possible through multiple radio reflections from the ionosphere and the earth's surface. Remote-sensing radar methods can be used to investigate the ionosphere. The ionosphere is scientifically important both in itself, as a tenuous ionised plasma coupled to the solar and terrestrial magnetic fields, which can support a number of plasma phenomena such as instabilities; and as a tracer, through collisional interaction, of the dynamics of the neutral high atmosphere. Harvey's was first and foremost a mathematician, and his early work involved solutions of the production function for the ionosphere. His work was mainly mathematical as he sought to understand the ionosphere by simulation. In the mid-60s his work on the conjugate ionosphere at low latitudes, using Raratonga and Hawaii data, found wide interest at the time.

A number of experimental radar methods exist for such investigations. Harvey was involved in the mathematical modelling of results from two such techniques: the ionosonde and meteor radar. An ionosonde sweeps a radar signal in frequency from 0.5-20 MHz over about half a minute, and records ionospheric echo traces as an archived (film medium when Harvey started) ionogram. These data can be reduced by standard methods to a profile of electron density as a function of height. Many morphological studies were made to determine electron layer parameters and their dependence on solar activity, season, and time of day, and rules for optimum radio propagation conditions were derived in part from these studies.

About half way through his professional life, Harvey wished to deepen his knowledge of hydromagnetic plasma waves, and studied for a Doctorate of Philosophy degree in Physics at Canterbury.

Harvey's ionogram work was principally with those ionograms that departed from the standard form. The inversion process of ionogram reduction is based on a number of assumptions, of which one of the most important is that of horizontal stratification. A dynamic, moving atmosphere can have time changes of the order of minutes and associated horizontal spatial scales of fifty to a few hundred kilometres. Such features alter the radio ray paths and can cause the ionogram to show features such as traces additional to those expected, "spread" in which the form of a trace is blurred, or the omission of parts of the trace ("lacunae"). Harvey first developed and published results on a fast ray tracing program. He then used this in a series of studies on the calculation of the ionogram traces to be expected from horizontally distorted ionospheres of various forms, with particular emphasis on the changes in the ionogram with alteration of the distortion parameters. It was possible to account for many observations by Harvey's models, indicating that the ionosphere at these times could have taken the forms assumed in the calculations.

The existence of such rapid ionospheric change and distortion begs the question of their cause. Throughout his life Harvey had a deep interest in the short-period atmospheric waves which are one cause of rapid ionospheric change, and in a series of papers and reports investigated how such waves distorted the ionosphere and the effects of such distortions on the ionogram traces obtained.

In his work on meteoric ionisation behaviour, Harvey modelled the evolution of the plasma irregularities controlled by diffusion in the presence of multiple chemical reactions.

Harvey's generosity to others will be remembered by all who knew him. During his time at the Geophysical Observatory, and later in the Physics and Astronomy Department, he was always willing to discuss new ideas and impart the benefit of his experience to co-workers, and to people entering atmospheric and ionospheric physics. It is important that our young students experience the wisdom and guidance of such luminaries as Harvey.

All of us, including many overseas visitors, will always recall the warm welcome to his home that he and his wife Helen always gave. We shared, for example, in his passion for cycling and enjoyed the many generous aspects of this warm-hearted man. We extend our deep feelings of loss to Helen, daughter Robyn, and sons Brent, Paul and Michael.

Jack Baggaley and Justin Cooper

2 COMMENTS ON THIS ISSUE FROM PHIL WILKINSON

This Bulletin starts out on a low note for me. A friend of many years, Harvey Cummack, passed away just over a year ago. For almost thirty years I enjoyed Harvey's special kind of humour and philosophy as he explained his discoveries in modelling the ionosphere and ionograms while not losing sight of the more important things in his life. I am glad of the time we had together and would have liked a bit more.

2.1 Publication Details: G5 Proceedings

Papers that have been accepted for publication in the G5 Proceedings will appear in a UAG report that should appear later this year, or early next year. It will be about the same length as UAG-103, which appeared after the last URSI meeting. The main details follow.

TITLE: Computer Aided Processing of Ionograms and Ionosonde Records.

EDITOR: P. J. Wilkinson;

all authors and INAG members will receive a copy.

2.2 Characteristics Scaled from Ionograms

At the Kyoto URSI General Assembly INAG Meeting, the problem of insufficient characteristics for recording data was raised. During the last triennium, a survey was made of the current characteristics and it was evident that there was no likelihood of recycling old ones. To solve this, we propose broadening the characteristics to include alphabetic, as well as numerical, symbols. A list demonstrating some new characteristics in given in the CHARS article later in this bulletin.

2.3 Data Availability

In the Lille report, I indicated that the WDC-A for STP was having difficulty obtaining current, and archive data from groups. Since the meeting, WDC-A now has obtained all the British data. However, French and Australian data are still not reaching the WDC. I hope this situation can improve further over the next year.

Professor Rishbeth raises a more serious issue regarding data availability. Somehow, scientific data has managed to come under the ambit of an effort to design legislation to prevent piracy of a wide range of computer software, including pre-recorded compact disk and cassette music. Unfortunately, by the time you read this, the decisions will probably have been made. While there may be commercial value in preventing the free distribution of data, I can see no legitimate scientific reason to support such legislation. Read this article carefully.

2.4 Leonid Meteor Shower

Bill Wright reminded some of us of the forthcoming Leonid meteor shower in November. Every 33 years, this annual meteor shower can reach meteor storm levels with visual meteor rates as high as 150,000 per hour. The next peak is predicted to occur in 1998 or maybe 1999, although there are good reasons for thinking no storm will be seen. An increase in meteor rates is expected in the years leading up to the storm year. During the 1966 storm, Bill reckoned he could see 100 visible trails at any instant. Although meteor rates were not high this year, it will still be worth watching out for this shower over the next two years, just in case. There are two articles in Sky and Telescope (November 1995, p24, November 1996, p74).

In addition, it is possible to observe the ionised meteor trail with an ionosonde, provided the ionosonde is sensitive enough and the ionogram is recorded in a short enough time interval (typically, within 10 seconds). Without careful calibration ionosondes are unlikely to offer good support for meteor science. However, during a major meteor storm they may recover enough data to be useful. This is a prospect worth further considering over the next year. Those interested in looking at some radio meteor results off the Web can go to http://allserv.rug.ac.be/~hdejongh/astro/meteor/meteor.html and successive pages. The University of Ghent radar is displays its observations directly to the Web.

2.5 Web comments

http://www.ips.gov.au/INAG This is the INAG Homepage that I have just created. Over the next two months, I intend adding items to it. I have material from past INAG Bulletins as well as the UAG Series articles and other assorted information. If you have addresses you feel might be interesting, notes you would like to see here, please email them to me at phil@ips.gov.au. Anybody who has a site they want referred to, or a favourite list of sites they find useful, please send me the information so I can collect then at our site.

There is good ionospheric information at a number of sites on the Web. If you are unfamiliar with the possibilities, a good start point is SPIDR. The Homepage is: http://www.ngdc.noaa.gov/ This is the interactive data request and viewing platform for WDC-A for STP, in Boulder, USA. A wide range of ionospheric data, as well as other data sets, is available at this address. For instance, the Web can reach ionosonde stations. In most cases near real time, data are available. Try http://www.noaa.gov/stp/IONO/grams.html, the SPIDR URL, for the links. Stations where there are digisondes are also available at: http://ulcar.uml.edu/framesd.htm.

The Japanese ionosonde stations are another good example. Go to http://wdc-c2.crl.go.jp The Homepage for the Communication Research Laboratories WDC-C2 for the Ionosphere. When you first log on you will find yourself on the Japanese page. Click on the English version, and then pass on to the "Ionospheric Sounding Data in Japan". There is a choice of ionograms and ionogram surveys and some nice data displays, including mpeg movies for November and December, 1997. All displays are current.

Some other ionosonde sites are:

http://www.irf.se/~ionogram/ where ionograms from Kiruna and Uppsala are displayed as movies and scaled data are presented in tables. You need to explore a little to find everything.

http://www.ips.gov.au/asfc/aus_hf/ion_cat.html is the IPS site for Australian real time ionosonde data. You will find the latest real time ionograms, as well as a catalogue of past hourly ionograms, for Hobart, Canberra, Sydney (also called Camden), Brisbane, Townsville, Darwin and, care of the University of Canterbury, Christchurch in New Zealand.

At http://www.ips.gov.au/asfc/aus_hf/index.html you can view the IPS real time propagation page. Here ionospheric maps based on the scaled ionospheric data are presented. This gives you some idea of how real time ionospheric data can be used.

There are many other sites. I hope this short list and brief comments will encourage you to send in further information. I am especially interested to hear of more ionosonde sites on the Web.

2.6 News from South Africa

Lee-Anne McKinnell (phlw@giraffe.ru.ac.za) offered the following comments:

"There is now a digisonde at Grahamstown and the data from the digisonde is available via anonymous ftp from our ionosonde server. The address is: ionosond.ru.ac.za

Scaled chirp sounder data is also available from the same site as well as from NGDC (Ray Conkright). If anyone has trouble getting into the server, they should e-mail me. The Other DPS ionosondes have been bought and are in South Africa. One of them has been installed at a station called "Madimbu". And it was put into operation last month, but there have been, naturally, teething problems with the remote connection and so there is no data available yet. Our third ionosonde is going to be installed at Louisvale, near Uppington, but it is far from being operational, as the site has only just been chosen. The ionosonde itself is at a test site in Pretoria until the installation date.

Our institute (Hermann Ohlthaver Institute for Aeronomy) also has a web page address now. The address is: http://phlinux.ru.ac.za/hoia/."

2.7 Computer scaling comparison

It is likely that within the next few years the majority of new ionospheric data flowing into data archives will be computer generated. The potential is there now, with increasing numbers of real-time ionosonde networks reporting data. Some groups have few, if any resources for manually checking the data they collect. In Australia, we still collect and manually scale large quantities of data, but our resources will diminish over the next decade.

If computer data proves reliable, then it will gradually replace manually scaled data as the primary data source. However, to date, there has been no substantial effort to identify and quantify the types of errors we should expect in computer generated data. Some individual scaling program errors have been reported, but there has been no attempt to quantify the likely errors from an ensemble of scaling programs. How good, or bad, can these programs be. Are there typical errors? Will knowledge of the likely errors enable us to define better operational methods? I think that the computer data is suitable for some purposes now, but it is not useful for research purposes and therefore unsuitable for archiving unqualified. That is why we have introduced the / scaling letter (see Reinisch this issue and INAG-58).

I now feel we need to go one step further with data comparisons. We need to compare the differences between the many scaling systems. This will give us some measure of the errors and types of error that are could become part of our data sets. It might focus

effort, it could act as a warning and it will certainly help define our future resources. It may, for instance, help us construct suitable arguments for more manual scaling.

I want to involve as many groups as possible scaling a selected set of ionograms. The main problem to overcome is that the different scaling methods often also use different ionogram formats. IPS is currently trying to solve this problem using a set of ionograms supplied by Tom Berkey. We plan to take a selection of mid-latitude dynasonde ionograms and construct other ionograms using the ionogram formats we are aware of to date. We will then make a CD-ROM of all the different ionogram formats and offer this to people to scale the ionograms. Requesting a copy of the CD-ROM means you will return your scaled values to me for comparisons.

I do not intend to compare different computer scaling methods. In fact, it is likely that several people could use the same programs to scale the ionograms. Such a comparison could be interesting, but it is a contentious issue. Instead, the object of the exercise is to make a first assessment of the range of errors that computer scaling imposes on the data.

At this stage, I am inviting anybody who is interested in participating in the exercise to contact me and register interest. I will look forward to hearing from you

2.8 New Address for IPS

In late September IPS moved to new offices. Our new address and contact details are:

IPS Radio and Space Services
P O Box 1386
Haymarket, NSW 1240
AUSTRALIA

Phone: +61 2 9213 8000
Fax: +61 2 9213 8060
IPS Homepage: http://www.ips.gov.au
My e-mail: phil@ips.gov.au

In all future correspondence, please use this mailing address.

In early December, I e-mailed many of you with these new details. I had great difficulty with some of the e-mail addresses, particularly those in Russia. If you did not receive e-mail from me, please e-mail me now so I can check the e-mail address I am using for you.

3 INAG MEETING: URSI GENERAL ASSEMBLY, LILLE, SEPTEMBER 1997
PHIL WILKINSON

Attendees

Matthew Angling	DRA-Malvern, UK
Ruth Bamford	Rutherford Appleton Laboratories, UK
Pal Bencze	Geodetic and Geophysical Research Institute, Hungary
John Bennett	Monash University, Australia
Josef Boška	Institute of Atmosphere Physics, Czech Republic
Peter Bradley	Rutherford Appleton Laboratories, UK
Mike Dick	Rutherford Appleton Laboratories, UK
John Goodman	TCI/BR Communication, USA
Rudi Hanbaba	France Telecom CNET, France
Robert Hunsucker	EET Dept, USA
Norbert Jakowski	DLR/DFD Fernerkundungsstatiojn, Germany
Jean-Claude Jodogne	Institut Royal Meteorologique, Belgium
Patrick Lassudrie	FT-CNET Lab, France
Reinhart Leitinger	University of Graz, Austria
Bengt Lundborg	Swedish Institute of Space Physics, Sweden
Allon Poole	Hermann Ohlthaer Institute, South Africa
Bodo Reinisch	University of Lowell, USA
Anil Shukla	DRA-Malvern, UK
Phil Wilkinson	IPS, Australia
Lee-Anne Williscroft	Hermann Ohlthaer Institute, South Africa

Two INAG Meetings were held. A short meeting was held to endorse the officers and a longer general meeting was also held to discuss issues that had arisen during the triennium. Because I was elected Vice Chair of Commission G, I had to stand down as Chair of INAG. I proposed Ray Conkright, of WDCA for STP, USA, as the new Chair of INAG and this was accepted by the meeting. I also proposed INAG would have two Vice Chairs and I was elected as one of these, together with Dr Jean-Claude Jodogne of Belgium as the second vice chair.

In my general report on the Working Group activities during the last triennium I made the following points. Over the last triennium the membership of INAG has remained constant, around 240 people with about 300 people on the email list. There were two INAG Meetings during the triennium and two bulletins were published as well as the UAG report produced from the Kyoto meeting session. The main issue raised during the triennium related to scaled parameters and is discussed below. Over the next three to six years the main issues are: establishing an INAG WWW homepage; build on the current email list for rapid communications and, most important, migrate to the digital environment without losing the integrity many correctly associate with manually scaled parameters.

The two main topics discussed at the second INAG meeting was: data exchange and scaled parameters.

Digital data is easier to exchange than the older analogue data, but, as Ray Conkright has pointed out, "Now that it is easier than ever to exchange data, we are getting less exchanged." Much of the current data exchanged passes through IUWDS (now ISES - International Space Environment Services) and arises from the USAF/DISS network. Ray pointed out, in a message to the meeting, that the WDC-A interactive data server, SPIDR, had little or no data from many locations e.g. no British data, little French data. This question was discussed at the INAG meeting. The British had no knowledge of the problem and promised to look into it and the French felt that while there may be a security issue with the real time data, they would probably be happy to supply archive data.

These appeared to be indicative of a general problem with data exchange. Several possible reasons were offered for the fall off in data exchanged. For instance, what are the problems associated with supplying data? Based on local experience, preparing useful archive data has several restraints: processing costs more; resources (people who know how) are scarce and available real-time data may make archive data less of an imperative. There have also been problems sending data to other groups: problems with the media (IPS is still having major problems exchanging data with the Russians); loss of autonomy (others use the data and offer no credit or insight into how they use it); and it costs money to send data to other locations. One suggestion was that ownership of current data should be protected and not just acknowledged. For instance, like other data sets, data should belong to the originating agency for the first two to five years. Pal Bencze pointed out that most of us know where data is used and therefore it is valuable to keep collecting it. However, it is worthwhile to once more remind authors that sending reprints to the stations whose data they use assists in defending the future of the station. To make this work, an up to date station address list is required. It is also important to remind authors to reference the Boulder CD-ROM. Others wondered whether people putting data into WDCA for STP would receive a free copy of the CD-ROM of data. There is also the almost trivial problem of not knowing if data reached its destination because often there is no feedback. There was general agreement that an acknowledgment that data has been received by WDCs is well worthwhile. People present agreed that some subset of these issues affected data supply.

What are the costs of losing WDC involvement? Has the old WDC philosophy gone? Over a decade ago, data were often regarded as a currency that could be banked with the WDC. In the mid-eighties, as data sets became more complex and far more expensive to prepare and distribute (for instance, incoherent scatter data, satellite and rocket data) a panel established to offer guidance on data centers proposed that being aware of where data could be obtained should be more important than actually holding data. The WDC role would be to help maintain a widely distributed data archive. Since scaled ionospheric data form a much smaller, labour intensive data set, it isn't clear this concept should apply. On the other hand, all data sets are vulnerable to funding pressures on Organisations so that ensuring the long-term survival of these data is better achieved through widely dispersed archiving. IPS has deliberately used the WDC as a back up for our data sets. How do others back up their long-term data? How easy is it for others to access this store?

How should data be made available: can WWW be compared with a CD-ROM? A CD-ROM comes as part of most children's games computers now. Consequently, the CD-ROM is almost a defacto standard for digital exchange media. WWW, on the other hand, although it can be more immediate, requires a large investment in time which can be greater for some countries than others. While WWW is great for browsing, a CD-ROM archive is far more appealing. Most agreed that for archiving, the CD-ROM is easier. However, WWW is a significant advance for handling real time and near real time data and will therefore always be more immediate. A combination of these is therefore necessary.

This discussion on data access and exchange was strongly endorsed by Working Group 4 (Ionospheric Informatics) as well as all at this meeting. However, although the problems were aired, it is hard to see any substantial changes arising. It is probably worth setting up an address list of known ionosonde stations and then send out a questionnaire asking them about their ability to record digital ionograms. Those that can supply data would be asked how frequently they record these data and whether they would be willing to store them in a WDC.

After the INAG meeting in Boulder (INAG-61) a survey was made to gauge the support for scaled parameters. The main reason for this was that some digital ionosonde groups were developing new parameters and were running out of numbers for coding them. I carried out a large survey of all the parameters and published a preliminary report in the last INAG Bulletin. The idea behind this survey was to discover if it was possible to abandon some of the parameters and reuse some of the codes. A subordinate objective was to correct any misunderstandings that existed among the current codes.

Questionnaires that are too long get few responses, and the INAG questionnaire was not an exception. However, although there have been only 15 responses so far, these have represented a wide range of opinions and backgrounds. The results are therefore indicative.

First, the current standard scaled parameters were all well supported, although three (h'F, h'E and fmin) each had one respondent suggest they should be abandoned. Because of the large amount of data already collected for these parameters, this is not feasible, but it suggests a little more thought about their long-term value is warranted. Surprisingly, two non-standard parameters, fzF2 and fxF1, were also reasonably well supported. A few parameters received reasonable support and with a little effort, these could also have the status of standard parameters. Of these, the IPS range spread (R/S) and frequency spread (F/S) parameters were surprisingly successful. Even with the IPS questionnaire returns excluded, these two parameters were well supported. This is surprising, as at IPS we have been considering discontinuing their use. All other parameters received mixed support and some, especially the spread-F parameters (h'I, fmI and M(3000)I), were unpopular. Unfortunately, there was no time for a detailed discussion of each of the parameters. For instance, the strong opposition to spread-F parameters, yet good support for R/S and F/S was worth discussion. Better coding for the presence of spread F is an important issue.

The reasons for wanting various parameters were much broader than I first expected. For instance, one person said they used many of the less familiar parameters as part of HF modelling programs. Another rejected the same parameters because they had no value for communications. The obvious conclusion of the meeting was that because of broad support it is not possible to recycle any of the current codes. A suggestion that three figures be used instead of two was accepted but has since been replaced by a decision to use alphabetic as well as numeric characters (*see later in this Bulletin*). This means that past archives will remain consistent with future archives.

While experiences people have had licensing ionosondes was going to be discussed, time ran out and since an allied topic was the subject of a resolution before the Commission, it was not pursued. The possibility of a session sponsored by INAG was also mentioned, but there was no substantial for it.

4 WILL WE STILL BE ABLE TO GET DATA ?

Henry Rishbeth, Department of Physics and Astronomy, University of Southampton, Southampton SO17 1BJ, U.K. (Phone: +44 1703 592073 Fax: +44 1703 593910 Email: hr@phys.soton.ac.uk Web: http://www.phys.soton.ac.uk/atmos/uagrp.html

31 July 1997

The long-standing tradition of "free and open access" to ionosonde and other STP data is under threat from legislation and treaties that are designed to meet the grave international problem of piracy of computer-based material, such as software, cassettes and compact disks. With the aim of solving this problem, treaties have been drafted by the World Intellectual Property Organization (WIPO), a Directive has been issued by the European Union (EU), and legislation is in course of introduction into the U.S. Congress. Similar measures may exist in other countries.

The European Union Directive 96/9 gives legal protection to "databases" (meaning collections of "independent works, data or other material arranged in a systematic or methodical way and individually accessible by electronic or other means"). Chapter II ("Copyright") protects the databases themselves, but the contents of databases - i.e. the actual data - are to be covered by a new form of protection, the "Sui generis" right (Chapter III). EU member states must implement Directive 96/9 by January 1998. They are permitted to allow dispensations for scientific and educational use of databases, but it is thought that the EU will press national governments to adopt a very restrictive approach that may well prevent scientists from freely using data in the traditional way - in particular, by collating and re-assembling data from a variety of sources. The "sui generis" right is especially worrying; it seems ill-defined, open-ended and all-embracing, and might be used to acquire property rights over long-established data sets that are widely regarded as being in the public domain. Moreover, restrictions may be placed on data exchange with countries that do not have similar laws.

The new "copyright measures" have many similar features:

- They are framed in very broad terms, potentially affecting many kinds of information, whether or not "electronic", "computer-based" or available "on-line".
- They may act retrospectively, to restrict access to old non-computerized data.
- They provide for royalties for any access to data (perhaps even casual perusal of data, with no actual "use"), with penalties for non-payment, unauthorized access, and use of protection-defeating devices.
- They prescribe terms of protection that are variously proposed as 15-25 years from the date of creation or of "substantial" updating, i.e. effectively in perpetuity.
- They make little or no provision for "fair use" or dispensation for scientific or educational purposes.

The scientific Unions have repeatedly advocated the principle of free and open exchange of data at minimum cost. This principle is based on the idea that data have no inherent commercial value. The present practice was formulated for the International Geophysical Year of 1957-1958 and has stood the test of time. It works to everyone's benefit. In general, the countries that contribute most to the system, by operating observatories and data centres, also make the heaviest use of data. It has never been considered worth trying to establish "gains" or "losses" in the data handling system. The data are archived in data centres and are freely available to scientists and engineers at minimum cost, largely through World Data Centres and FAGS Centres. For their part, most research scientists are generous in allowing others to use their data.

The new copyright and "sui generis" measures, with their emphasis on "rights" and "payment", raise the spectres of a commercial "data market" and of "intellectual property rights" in scientific data. These risks are greatest where (as increasingly happens) data operations are privatized or contracted out. The consequences may be especially serious for science in developing countries, which are least able to meet the cost. It should be noted that the "fair use" dispensations from "sui generis", that may be given by national legislation, will not necessarily allow scientists to collate data from different databases, in the manner in which so much ionospheric research depends.

The concept of a commercial "data market" (ideologically attractive to some politicians and

economists) threatens long-term and academic research. Since practical benefits of research may not appear for some years, it is extremely difficult either to attach monetary value to the data or to recover the great costs of acquiring and archiving data - even supposing there is any real advantage in so doing. In consequence, cash-limited projects are forced to use fewer data, even if the science requires more. Measures for "cost recovery" (e.g. "pay-per-use" systems) lead to a situation in which short-term commercial value becomes the only criterion for collecting data. Long-term research becomes difficult or impossible, and environmental trends may go undetected.

In STP and some other branches of science, it is highly doubtful whether "cost-recovery" ever works. It merely recycles and dissipates funds between users and funding agencies. Its inevitable administrative burdens are mostly borne by the scientists. As these burdens are not highly visible, managements may ignore them in order to make the "cost recovery" appear spuriously "profitable": it is not difficult to conceal $50's worth of work consumed in selling $10's worth of data.

The scientific community must act to ensure that its work can proceed without new legal, administrative and financial burdens. It is vital to maintain a "public domain" in scientific data and data services, free of individual property rights, and to ensure that data in this public domain remain freely and openly accessible. Agencies that support scientific research, such as NASA, NOAA, ESA and counterparts in other countries, should be asked to affirm or re-affirm that data obtained with their funds will be subject to free and open access (with allowance for reasonable time-limited "first use" privileges where necessary). Some treaties and agreements already provide "free and open access"; they should be exploited. Reasonable objectives are:

- To press national governments, the European Community and WIPO for reasonable "fair use" provisions for scientific and educational use of data, that are sufficiently wide-ranging to allow the collation and assembly of data from diverse sources, in the manner that is essential to the progress of astronomical, solar-terrestrial, geophysical and environmental science;
- To ensure that existing and future scientific data, of kinds that are currently in the public domain, continue to be openly available at minimum cost and formality, without hindrance from copyright or property rights.
- The copyright measures may make more urgent (and difficult) another STP necessity: To ensure the continued collection and archiving of basic monitoring data in the 21st century, both to support ongoing research and to enable study of long-term change.

Time is short! Acts, Treaties and Directives will be imposed soon! Try to find out the situation in your own country, and do your best to influence it!

5 POLAR LACUNA – A SINGLE DESIGNATION FOR VARIOUS GAIN-SENSITIVE PHENOMENA

By J K Olesen, Senior Scientist, Dag Hammarskjolds Alle 21, DK 2100 Copenhagen, Denmark

Abstract

While the source and characteristics of the E-F Lacuna ionograms have been reasonably well established as an effect of an E-region plasma instability causing the so-called Slant E Condition (SEC), it seems that the F2 lacuna concept as defined in the Dumont d'Urville ionograms is still on a more debatable level. The present note emphasises the gain-sensitive character of lacuna and demonstrates how this fact – in combination with the ionogram interpretation practice used – make the Dumont d'Urville F2 lacuna occurrences a mixture of several unrelated factors. This might make it desirable to reconsider the F2 lacuna concept and possibly split it up into groupings with more homogeneous sources.

5.1 Introduction

Reference is made to 2 previous LETTERS to the Editor in ANNALES GEOPHYSICAE on the subject: Polar lacuna on ionograms, i.e. Cartron and Vila (1994), and Stauning (1995) including a responding Note: by P. Vila. The main theme in the discussions concerns the nature and relationships of various types of lacuna on ionograms. In the present note, the main theme shall be on an F2-region lacuna (lack of F2-echoes only) contra what here shall be called on the E-F lacuna (lack of echoes from the

upper E-region through part or all of the F-region) – called E- region lacuna by Stauning, and L1 or L3 lacuna respectively, by Cartron-Vila. In my notes below I present various assumed conditions for the definition of Dumont d'Urville F2 lacuna and its observation as the necessary preconditions for its existence.

It is a special pleasure for me to comment on this subject, which I have been involved in for more than 40 years of experimental and theoretical activities, and – of special importance in the present context – including 7 years as operator of ionosondes at one-man operated ionosonde stations at various latitudes from the auroral Zone to the geomagnetic polar regions.

I agree on the statements in Stauning's Letter. They are along the lines of previous studies, that I have been involved in on the subject – all the way from the very first identification of the E-F lacuna, (Olesen, 1957, Olesen and Rybner, 1958) then called the "height interval of missing reflections" or "the E-F frequency gap", and described as an "appendix" to the associated slant Es phenomenon, since that was the only phenomenon of the two identified before that time. In particular I agree on Stauning's recommendation on a very strict discrimination between cases of F-region lacuna, with or without E-F lacuna, respectively.

As to the Cartron-Vila Letter and the Vila Note; I refer to the discussions below on the various aspects.

5.2 On The Dumont d'Urville F2 Lacuna Concept

In their hope of reaching an agreement on our different viewpoints on the lacuna, and in particular the F2 lacuna concept, I shall below discuss the main features related to the Dumont d'Urville F2 lacuna concept, as I have understood them. My goal is to reach a common basis for interpretation of lacuna ionograms, or at least to be aware where our standpoints differ. Unfortunately original Dumont d'Urville F2 lacuna ionograms, so important for the discussions, are rather seldom shown, but a few have been found as referred to below.

5.3 Occurrence Of F2 Lacuna At Dumont d'Urville

The occurrence of F2 lacuna at Dumont d'Urville is tabulated not only when the F2-echoes are completely missing at maximum system sensitivity, but also when the F2 echoes are weak or absent at the existing gain setting and overall system sensitivity – even if one or both of them might be low. This impression is stressed by using the term "F2 quasi lacuna".

Documentation/discussion on these statements may be found e.g. In the following reports: Cartron et al. (1971, fig 4 and 6), Cartron et al. (1972,PL24), Olesen (1980), Sylvain (1972), Sylvain (1979, fig.1), Sylvain et al. (1978). The effect of gin setting is illustrated e.g. in figure12.2 in Piggott (1975). See also Rodger (1989), whose figure 1 and table 1 illustrate a unified model for E-F lacuna and F2 lacuna. My main reservation is, that if there is not a G-condition (see below), then in reality the F2-echoes do not disappear as it might be indicated in Rodger's figure, they just weaken. At sufficiently high system sensitivity they show up, maybe somewhat disordered with spreading and obliques, but echoes from the F2-region are there. But naturally, if the French definition of lacuna described above is accepted, we may call it an F2 lacuna under these circumstances.

My further comments: If the above conditions, stated for Dumont d'Urville F2 lacuna, are correct and accepted, I agree on its existence. My reservation is that this will imply the mixture of several unrelated conditions under the lacuna concept. Such as low F2-reflectivity for some reason: tilts, blobs, spreading and other irregularities, and in addition: absorption of the F1 deviative type, when foF2 is little above foF1, probable during SEC events, when some R-region absorption might also add to F2-echo attenuation. Also D-region absorption might contribute, and maybe worst of all; low system sensitivity might be misinterpreted and tabulated as F2 lacuna. See further remarks in next paragraph on system sensitivity.

5.4 G-condition

G-condition (F2 electron density less than underlying layer densities) is only tabulated at Dumont d'Urville when the succession of ionograms clearly demonstrates a gradual decrease of foF2 towards underlying layer densities. Also, it is presumed that a substantial change of foF2, in less than one minute, is not possible. So when an F2-echo disappears that fast, a G-condition interpretation is excluded. All cases of F2-echo weakening or disappearance that do not satisfy these requirements for G-condition qualification are tabulated as F2 lacunae. It is emphasised that the above criteria are evaluated on the basis of ionograms recorded with the system sensitivity that happens to be there at the time in

question – even if that system sensitivity might be low at the relevant frequencies.

Documentation: Sylvain (1979, figure 3). See also Rodger (1989) on foF2 decrease tendency during lacuna, and Sylvain (179) on foF2 decreases as a general tendency during magnetic storms and thus during SEC.

My comments: I do not agree with the 1-minute reservations about foF2 changes indicated by Dr. Sylvain. Changes of F2 electron density during SEC are not necessarily of the normal rather slow recombination type, cf. e.g. Rodger (1989). Also the appearance of an F2-trace, when foF2 decreases towards foF1, requires an extraordinary height system sensitivity at the frequencies in question (due to foF1 deviative absorption – and maybe E-region absorption), cf, the Handbook recommendation on the use of high-gain recording for reliable G-evaluation (Piggott and Rawer, 1972). High sensitivity was not present in the Sylvain (1979 figure 1 and 3) illustration, cf. the lower noise levels at 2.25-6.75 MHz revealing lower system sensitivity through that band. The "Magnetic A/B, 1005W" ionosonde used has a special weakness in that the receiver has 3 bands, which are individually tuned, and there are difficulties at attaining a flat sensitivity curve over the frequency bands. Especially band 2 covering the – in the present context very important-frequency band 2.25 to 6.75 MHz is difficult, which is evident in the referred figures. That problem was a main reason why we – after many years of extra care and troubles – exchanged our "Magnetic" ionosonde at Godhavn with a "C4", which has a broadband receiver without that complication. This sensitivity problem might – in addition to antenna characteristics – contribute to the surprising scarcity of slant Es cases reported at Dumont d'Urville during E-F lacuna occurrences, cf. King (1971).

5.5 Other Comments on the Cartron-Vila Statements

The argument for the F2 lacuna existence, that its daily occurrence distribution is similar to that for E-F lacunae (ref. their figure 3), is not very weighty. The similarity would be there, if the F2 lacuna class was created partly by misinterpreted G-conditions, partly by cases, where the E-F lacuna of F1 deviative absorption might be the last "drop" of attenuation needed to reduce the F2-echo strength sufficiently for the authors to tabulate an F2 lacuna. This might be with the existing – maybe low – system sensitivity through the frequency band in question, in a situation, when foF2 is likely to be little above foF1, so that F1 deviative absorption might be considerable. Cases with other causes for low F2 echo signal strength might be those, that widens the curve for L2-occurrence beyond MLT-hours for L1 and L3 as seen in figure 3.

With reference to some critical remarks in his Note, I can assure Dr Vila and all other users of the High Latitude Supplement (Piggott, 1975), that they can be confident on its description of the main features of SEC, the E region phenomenon responsible for the slant Es trace as well as the E-F lacuna. It is stressed, that when the term SEC is used to describe the configurations in the ionogram, it covers both of them-or any one of the two, depending on which of them is absent for some reason. Linguistic formulations sometimes seen where "SEC" is co-ordinated with "lacuna" is thus irrelevant and confusing and should be avoided. The combination in the SEC concept of both slant Es and lacuna is very important due to the "opposite" gain-sensitive character of the two (E-F lacuna increases and slant Es decreases at low sensitivity, ref. e.g. figure 12.2 in Piggott, 1975). The SEC concept thus gives a "double" check on the evaluation of the ionogram. Another important consequence of slant Es-lacuna coupling as done in the SEC concept is, that it gives the only chance to reveal E-region heating events in ionograms, when there is no F-layer to reveal a lacuna; just a slant Es trace attached to a sporadic layer – often of the totally blanketing auroral type (Olesen, 1972). These events may occur at night and in winter, primarily at auroral zone stations like Tromso and Narsarssuak – and in very rare cases, at high latitude stations like Godhavn (and Dumont d'Urville?), when auroral activity happens to move up there, see Piggott (1975, fig.12.5 and 12.6) and Olesen (1989, fig. 2 and 3).

5.6 Conclusion

In summary I agree on the existence of an F2 lacuna phenomenon, if the various preconditions above an accepted, especially "weak F2 traces" and "low equipment sensitivity".

I personally would have preferred another designation for the F2-echo weakening. In particular, a more reliable evaluation of G-conditions, when no F2-echoes are there, e.g. by acceptance of the Handbook recommendation on high gain records for G-evaluation. Also, I would have preferred weak F2-echoes characterised e.g. by letters like R (attenuation in vicinity of critical

frequency) or C (interpretation impossible for non-ionospheric reason, or equipment failure), so that the Y designation might have been reserved for the daylight E-F lacuna, where a clear unavoidable gap occurs even at absolute maximum system sensitivity due to the excessive amount of absorption present. Based on incoherent scatter measurements during an E-F lacuna event the attenuation of lacuna frequencies between 3 and 3.8 has been calculated to be 22 to 61 dB (Stauning, 1984, Stauning et al., 1985, Olesen et al., 1986).

In fact, the above complications might be reduced if the recommendation on the use of height gain records was prescribed and obeyed, not only for G-evaluation, but for all gain-sensitive phenomena including the lacuna phenomenon; at least, for data used in research.

I appreciate very much the continued studies of lacuna and associated problems. I hope my comments above may help in our efforts to unveil the final full story on the lacuna and related phenomena.

References

Cartron, S., C. Davoust, G.Pillet and M. Sylvain, F-Lacuna, INAG Bull. No. 9, 5-9, WDC-A for Solar Terrestrial Physics, Boulder, 1971.

Cartron, S., C. Davoust, G. Pillet and M. Sylvain, Interp retation d'ionogrammes de haute latitude (Dumont d'Urville, Terre Adelie), Contribution francaise a la reunion du Groupe-Consuil du reseau ionospherique (INAG), Varsovie, PL.24, 1972.

Cartron, Suzanne, and Paul Vila, Polar lacuna on ionograms, I: Brief morphology, Ann. Geophys., 12, 355-358, 1994.

King, G.A.M., Letter to Madame Cartron, CNET., INAG Bull. No. 6, p.18, WDC-A, Upper Atmosphere Geophysics, NDAA, Boulder, 1971.

Olesen, J.K., Slant Es ionospheric disturbance at Godhavn and its correlation with magnetic activity, Ionosphere Laboratory Report RIA, Copenhagen 1-17, 1957.

Olesen, J.K., On the polar Slant E Condition, its identification, morphology and relationship to other electrojet phenomena, AGARD Conference Proceedings, 97, 27.1-27.19, ed. J. Frihagen, 1972.

Olesen, J.K., Lacuna, SEC problems, INAG Bull. No.31, p.19, WDC-A for Solar Terrestrial Physics, Boulder, 1980.

Olesen, J.K., P. Stauning and R T Tsunoda, Radio Science, 21, 1, 127-140, 1986.

Olesen, J.K. Coments on 2 articles on lacuna by Suzanne Cartron and Paul Vila in INAG Bulletine 52, INAG Bul. No. 54, p.9, WDC-A for Solar Terrestrial Physics, Boulder, 1989.

Olesen, J.K. and J. Rybner, Slant Es disturbance at Godhavn and its correlation with magnetic disturbance, with Appendix: Note on the occurrence of slant Es at Narsarssuak, AGARDograph 34, 37-57, 1958.

Piggott, W.R. High-Latitude Supplement to the URSI Handbook on ionogram interpretation and reduction, Report UAG-59, 227-239, WDC-A for Solar Terrestrial Physics, Boulder, 1989.

Stauning, Peter, Absorption of cosmic noise in the E-region during electron hearting events. A new class of riometer absorption events, Geophys. Res. Lett., 11, 1184-1187, 1984.

Stauning, Peter, Polar lacuna on ionograms, E-or F-region processes 7, with Note by P. Vila, Ann. Geophys. 13, 450-453, 1995.

Stauning, P., J.K. Olesen and R.T. Tsunoda, Observations of the unstable E-region in the polar cusp, in J.A.Holtet, and R. Egeland (eds.), The PolarCusp, 365-376, D. Reidel Publ. Comp. 1985.

Sylvain, M., Etude du phenomene lacuna a la station Dumongd"rville, These, Lab. dE Geophys. Ext., St. Maur,France, 1972.

Sylvain, M., J.J. Berthelier, J. Lavergnat and J. Vassal, F-lacuna events in Terre-Adelie and their relationship with the state of the ionosphere, Planet. Space Sci., 26, 785-699, 1978.

Sylvain, M., F2 lacunas and G condition, INAG Bull. No.29, 12-17, WDC-A for solar Terrestrial Physics, Boulder, 1979.

6 UPDATED SOFTWARE FOR IONOGRAM RECORDING AND ANALYSIS.

J.E. Titheridge, Physics Department, The University of Auckland, Private Bag 92019, Auckland, New Zealand.
email: j.titheridge@auckland.ac.nz.

6.1 "Digion" Ionogram Data.

The popular KEL IPS-42 ionosonde can be controlled by a microcomputer, to obtain digital ionograms. The data are commonly stored on magnetic tape cartridges. Unfortunately this medium has proved unreliable, with some cartridges producing numerous tape errors. With the compressed tape format normally used (and the compressed nature of the basic data), one error makes the remainder of the file unreadable. A new computer program FIXION has been developed to scan daily ionogram files and report any errors. The program can then be used to find all useable ionograms and write them into a new, uncorrupted, file - this typically saves over 95% of the data. The source programs Fixion.c, and a compiled version Fixion.exe, have been placed in a DIGION subdirectory of the ftp site set up by IPS, at ftp.ips.gov.au/users/phil/digion

Updated versions of the program Digion, used for viewing and scaling the ionogram data, are also available from this site. A further utility Dignum has been produced to change the site number on all ionogram files, if required, and to set a fixed "offset" that may be desired to correct for receiver delay, etc. The operation of all programs is summarised in a Readme file. Further programs to produce real-height profiles directly from the scaled data, using the program POLAN, may become available in 1998.

6.2 "Digion" Hardware

There may be some who are still using a KEL IPS-42 and storing the ionograms on film – or who have stopped recording, because of the cost and inconvenience of film records. You should note that the hardware and software for using any simple P.C. to control the ionosonde, and collect accurate digitised data at any required intervals, is still available from the author. The equipment consists of a plug-in board for the computer, a small board that wires into the rear of the ionosonde, all necessary cables and connectors, full software (with source code) and instructions. The full system costs US$1600, and can be used with most 'obsolete' computers (286 or later). For high-resolution ionograms recorded at 5 min intervals, storage requirements are about 1MB per day. Thus a single 100 MB ZIP cartridge will hold all data for six months, using normal data compression, giving reliable storage and fast access. For further information on this system, used at over 20 sites around the world, contact me or see the articles in INAG-60 (Nov. 1993) or UAG Report 104 (from the World Data Centre A).

6.3 Real-Height Analysis Using "Polan"

Minor updates have been made to POLAN over the last several years, and a larger revision (primarily to improve the model valley assumed between the E and F layers) is planned for mid 1998. All of the POLAN programs are also now available on the IPS site, at ftp.ips.gov.au/users/phil/polan. Anyone using a version without the December 1995 updates (as described at the beginning of POLAN.FOR) should obtain the new files. Again could users experiencing any problems please email me with copies of the offending data and the corresponding output. The programs have been well tested, over many years, but every data set is different and feedback is essential to make improvements and help with problems. Thus one group recommended to others (but not to me!) that frequent bombs made POLAN unusable with x-ray data; I found later that ALL their bombs were due to a faulty copy of POLAN. Don't let this happen to you!

Use of the IPS site for ftp transfers should make it much simpler for people to obtain copies of the latest programs, and I am most grateful to Phil Wilkinson for making this route available.

Note from Phil Wilkinson: if you have problems using the ftp site, please send me e-mail at phil@ips.gov.au.

7 OBLIQUE SOUNDING IN AUSTRALIA

K.J.W. Lynn
Ionospheric Systems Research, 34 Gallery Rd, Highbury, Australia SA5089
email: kenlynn@senet.com.au

7.1 Introduction

While oblique ionosondes have operated for a long time, scientific study and routine monitoring of the ionosphere has mainly been conducted with vertical ionosondes.

Improvements in the personal computer, the advent of GPS timing, stable synthesizers capable of rapid frequency changes and stable frequency sources has resulted in a new breed of flexible ionosonde where the format of the sounding is under computer control and both pulse and frequency-swept (FMCW) operation is available. The use of oblique sounding has become an option to an extent not previously seen. This article explores some of the characteristics and applications of oblique ionospheric sounding now made available as illustrated by oblique sounding in Australia.

7.2 Equipment

Results discussed here were initially derived from a type of oblique ionosonde built within the Australian Defence Science and Technology Organisation (DSTO) for research purposes. This equipment has been effectively deployed since the early 1990s (Clarke etal, 1993). These ionosondes trade a comparatively long duration frequency sweep for low power of operation (<50 W) and were originally developed because of the high cost and limited flexibility of the commercial oblique FMCW (chirp) sounders then available. However these ionosondes use the standard commercially available waveform and can operate in conjunction with such equipment. FMCW rather than pulsed operation is preferred for long-range oblique operation because of the low power required and high sensitivity obtained. Conventional pulsed oblique ionosondes of a past generation typically operated with peak powers of 40 KW or more with all the problems and costs such high powers generated..

A frequency range from 2 MHz up to 64 MHz was needed to cope with the high maximum frequencies seen on long, one-hop low latitude paths at sunspot maxima. Frequency sweep rates from 100 kHz/s to 500 kHz/s (or higher) were made available and successively employed for reasons described later. Transmitters and receivers were built in separate racks and could be operated separately or together at the one location.

Rubidium frequency standards were used to eliminate relative oscillator drift and GPS timing successively added to allow absolute timing synchronisation of ionosondes many thousands of kilometres apart and thus the group propagation time delay over the path. Each receiver could be programmed to receive a number of transmitters with a variety of sweep rates and frequency ranges tailored to the path in question.

The Australian ionosonde manufacturer KEL Aerospace has developed a number of additional options to their commercially available IPS-71 ionosonde finally arriving at a system which can pulse vertically for conventional or fast Doppler ionograms while also able to both transmit and receive the conventional oblique wave-form for complete compatibility with the DSTO ionosondes. The IPS-71 is now operating in conjunction with existing DSTO oblique sounding equipment.

While results discussed here were obtained specifically with the above equipment they should be regarded as indicative of what can be obtained with modern ionosondes although specific results will depend on the quality of the equipment (eg receiver sensitivity and antennas)

7.3 Antennas

At a distance less than 1500 km, the normal crossed-delta antenna commonly used by existing vertical ionosondes has been found to be effective in oblique operation despite the poor gain at low elevation angles inherent in such a system. Figure 1 shows an oblique ionogram obtained over a path of 2105 km by an IPS-71 in conjunction with a DSTO transmitter operating on a routine basis at the high sweep rate of 500 kHz/s and 10-20w . Existing crossed delta antennas are used at both sites. Such operation is at the limit of scientifically useful reception over a 24hr period as indicated by the high noise background and presence of the horizontal line generated by internal ionosonde noise which becomes apparent at the limit of receiver sensitivity.

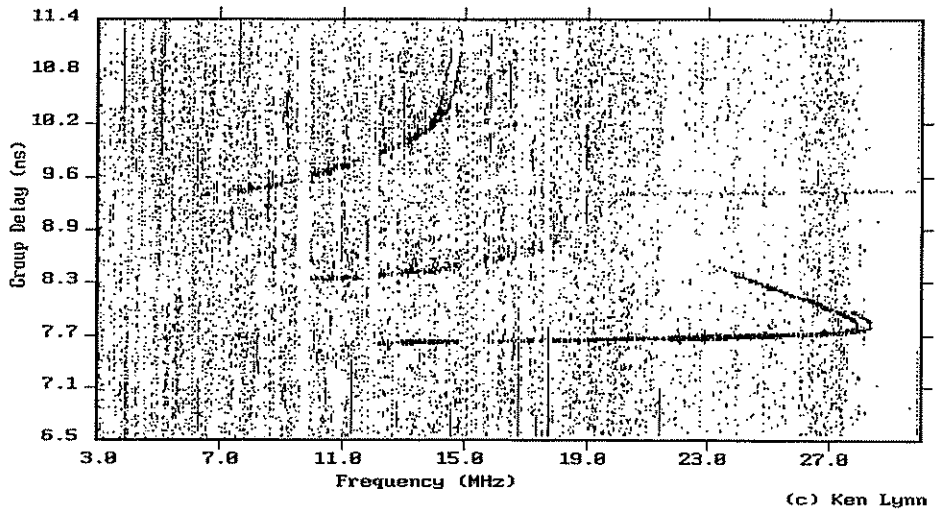

Figure 1. Oblique ionogram, 2105 km path, 500kHz/s sweep rate

The extent of Spread F, for example, becomes very difficult to recognise under such conditions.

At ranges greater than 1500 km, low launch antennas are increasingly essential. The choice here is between directional and non-directional antennas which is best determined by the application. For omni-directional reception at long ranges, some form of vertical monopole antenna is required in a simple system. Broad band antennas capable of operating over a 4-64 MHz range are not available and recourse must be made to a suite of antennas. DSTO has used a three or four antenna combination of a low frequency and mid-frequency vertical monopole and one or two high frequency yagiis for frequencies above some 25 MHz. The ionosonde equipment (both transmit and receive) operates with an internal programmed switching unit which switches the transmitter to the desired antenna at different stages of the sweep.

The minimum range an oblique FMCW ionosonde has been routinely operated by DSTO over flat terrain has been 11 km between a vertical transmit delta and a horizontally polarised dipole with both aligned to minimise reception of the ground wave so as not to overload the receiver. This quasi-vertical system provides the equivalent of a vertical ionosonde. Such expedients are no longer required when using a single ionosonde which can handle both vertical and oblique operation.

7.4 Ionosonde Programming

The basic limitation in running a sounder with a program of vertical and oblique sounding/reception is one of time. At the original rate of 100 kHz/s, an oblique ionosonde sweep over a 2-30 MHz range takes nearly 5 minutes. This is barely acceptable in taking a "snap-shot" of the ionosphere. At a 15 minute sounding rate this would allow the monitoring of up to three oblique paths and another 4 vertical soundings just might be squeezed in. To cover a 4-64 MHz range at this rate would take a prohibitive 10 minutes/ionogram.

The solution is to go to a higher sweep rate. In this case the ionogram is completed in a shorter time but with some possible degradation in quality. Only experience with a specific ionosonde and antenna system will provide the optimum trade-off between ionogram quality and sweep rate. With the equipment discussed above, 250 kHz/s sweeps were found to provide acceptable quality if antennas were suitable to the path length (up to 3000 km). However to increase the number of paths monitored it was sometimes necessary to go to 500 kHz/sec (as shown in Figure 1) with the proviso that path lengths at such rates be preferably kept to less than 1500 km. At this fast rate, a 28 MHz range is completed in less than 1 minutes and a 60 MHz range in 2 minutes. Some additional time may be taken in processing the ionogram but this should be small compared to the sweep time.

7.5 Oblique Ionosonde Applications

All applications listed below require accurate measurement of group time delay over the propagation path except for (a).

(a) Propagation Prediction Testing. This was the original requirement met by the DSTO oblique sounding program (Clarke etal, 1993). Many codes are available today to provide propagation predictions for HF users. Such codes are usually based on a database of measurements of foF2 and M(3000) or related phenomena derived from vertical sounding. Such programs achieve their greatest accuracy at shorter ranges. However little validation

has been carried out (or is indeed possible) over long ranges and in all geographic circumstance. For this purpose, oblique sounding is imperative.

Whereas the upper frequency limit for short-range propagation (<500 km) is set by the maximum density of the ionospheric profile, the maximum frequency available for the F region over an oblique path is sensitive to both ionospheric critical frequency and height and in consequence suffers a greater variation than is familiar to operators of vertical ionosondes. The absence of direct comparisons may leave engineers and other users with entirely unrealistic views as to the variability and predicability of long range reception.

(b) Direct Range Conversion. This is a technique long known (Davies,1965) but little used which becomes of particular value as a direct method of converting oblique ionograms to an equivalent ionogram for any chosen range. The author considers this simple technique as the key to the full realisation of the potential of networked oblique ionosondes (Lynn, 1995). It has the great virtue of using all the experimental data available in an ionogram while dealing with both height and critical frequency changes without resort to modelling assumptions inherent in prediction codes. A limitation is that it is only effective for the o-ray and has a small but defined error (largely removed by the k factor).

(c) Ionogram Inversion. Methods for converting a vertical ionogram into an electron density profile have been developed over the last 30-40 years and have reached a high degree of accuracy and acceptance with programs such as POLAN in common use. Methods for inverting oblique ionograms have received less attention and have yet to achieve widespread acceptance. In Australia, a program called OBLINV (Phanivong, etal, 1995) has recently been developed. This has proved capable of producing excellent results on test oblique ionograms for paths less than some 1500 km but has yet to be tested over a wide range of oblique ionograms.

An alternative inversion technique is to convert the oblique ionogram into an equivalent vertical ionogram and then process this ionogram using a vertical inversion code. Again not enough testing has been done to demonstrate a wide-ranging capability. Poole (1995) has suggested other methods and there are many possible variants.

Whatever technique is used runs into the problem of increasing time delay compression inherent in an oblique ionogram. A vertical ionogram which extends over 4 ms will be reduced at some range to less than 2 ms with the greatest compression at the lowest heights. The oblique ionosonde does not have the time delay resolution to enable these lower levels to be expanded to equivalent vertical values without a major degradation in measuremental accuracy. Beyond some 2000 km the E region will be cut-off altogether losing all hope of accurate direct reconstruction. At long ranges a hybrid system employing model values for the lower layers is required to obtain an electron density profile estimation.

On the positive side, the delay compression means that an oblique ionogram covers a greater effective height range than the usual vertical ionosonde setting which becomes of particular value during ionospheric storms or when other large increases in virtual height occur. Such events may lift the virtual F region trace beyond the normal range of a vertical ionosonde.

(d) Networking. The recent rapid improvement in data communications makes the networking of ionosondes an important step in providing ionosonde data to those who need it in real-time or near real-time. The constant battle to prove the ongoing relevance of ionosondes can be greatly assisted by developing techniques to meet the needs of a potentially new generation of users. In this regard, a network of ionosondes linked directly to a central location is an important step in the immediate distribution of raw or processed data to both civil and defence users of HF as well as for scientific study.

Such a system should be regarded as an ionospheric weather service with as much relevance to HF and satellite communications (as well as GPS and OTH Radar) as a tropospheric weather service to surface applications. (For a general overview of ionosonde networking and where it has currently been achieved see UAG-104, 1995 in References.) Digital data transmission over phone lines is continually decreasing in cost but the INTERNET may provide the ultimate system for the cheap collection and distribution of ionosonde data. Some initial examples are already on the World Wide Web and can be considered pioneers in this field..

The advantages that fielding combined vertical and oblique ionosondes can provide when networked are illustrated in Figures 2(a) and (b). Figure 2(a) shows a hypothetical distribution of eight vertical ionosondes deployed so as to provide an ionospheric weather service over the

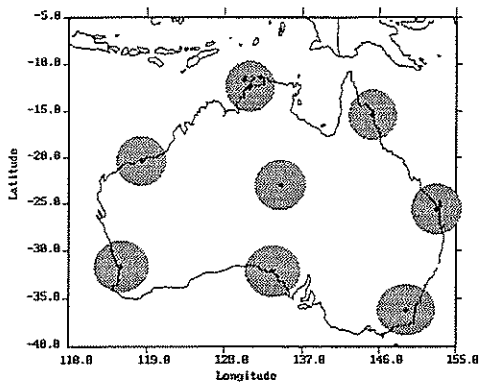

Figure 2. (a) Coverage achieved with vertical sounders

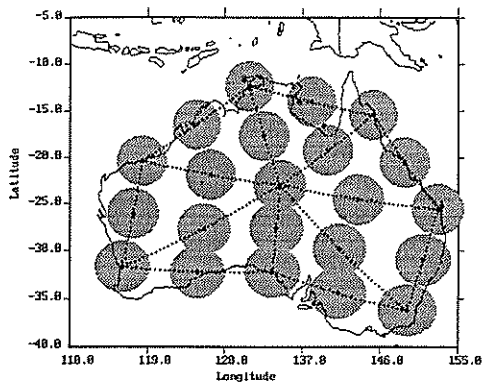

Figure 2. (b) Coverage achieved with vertical/oblique sounders

continent of Australia. (If such a number seems large it should be noted that there are more than eight ionosondes operated in Australia by a variety of independent users but with as yet no major effort to rationalise and integrate them. One suspects that similar conditions exist in other countries.) The circles with a radius of 300 km drawn around the vertical ionosonde reflection points indicate the area of high F region correlation. It is evident that the continental area is very much undersampled by such a distribution if an accurate mapping of ionospheric conditions is desired.

Figure 2(b) shows the coverage achieved if these same eight ionosondes are able to operate obliquely as well as vertically. By allowing each ionosonde to receive and transmit to its closest three neighbours, the number of reflection points being monitored has increased to 24 and the continental area is now well covered.

A major objection to the use of oblique sounding is that the information contained cannot be readily be integrated with that obtained by a traditional vertical sounder. This is not so. The use of direct range conversion as mentioned in (d) can convert ionograms from a mixed distribution of vertical and oblique paths of differing length to a common effective range (as can ionogram inversion combined with ray-tracing, if such can be made reliable). Moreover this removes the last vestige of undersampling by allowing the development of an integrated picture within which spatial interpolation can be carried out to counter the effect of large-scale gradients across the area of coverage.

When used for real-time frequency management it is thus possible to convert all ionograms to the range of the communication link and spatially interpolate the picture to the reflection point of that circuit.

By way of illustration, consider the two pictures shown in Figure 3(a) and 3 (b). Here a group of oblique ionograms (and vertical ionograms from

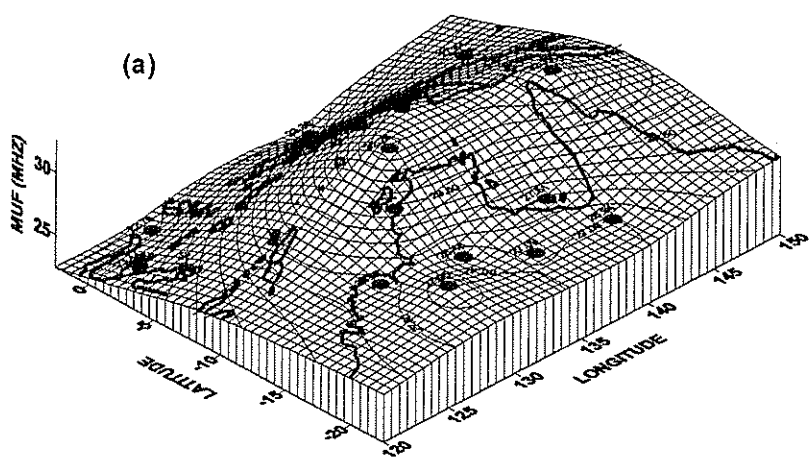

Figure 3. Spatially interpolated maps of MUF normalised to a path length of 2000 km (a) 0600 UT

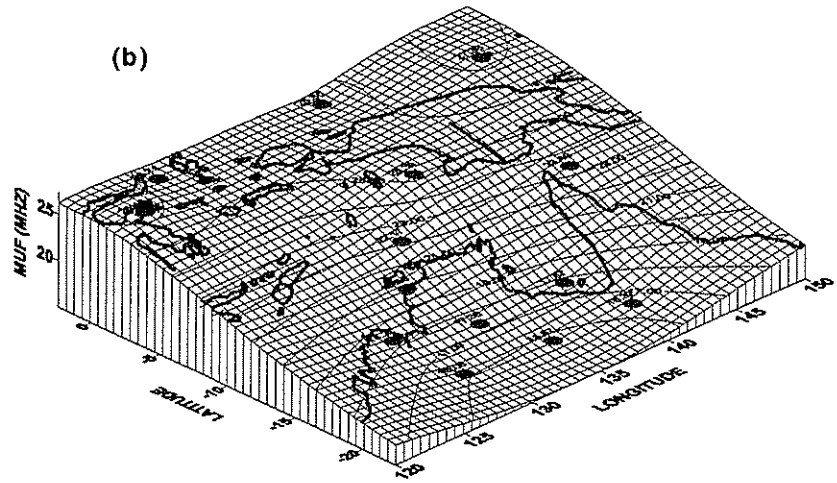

Figure 3: (b) 1200 UT.

Darwin), representing sparsely sampled snapshots of the low latitude ionosphere, have been range-converted (in this case to 2000km) and combined by the Kriging spatial interpolation technique (Samardjiev etal 1993) to show the effective maximum frequency for a path of this length reflecting anywhere in the sampled region at the time in question. Figure 3 (a) shows the development of the equatorial anomaly whereas Figure 3(b) shows the major north-south gradient which occurs at a later time of day. The round spots within the picture show the apparent location of the oblique reflection points (oblique path mid-points) used in the interpolation.

It is obvious that such a mapping technique can have both scientific and practical application. In the former case, it can be used to compare the actual ionosphere with predictions generated by computer codes. If all sites are connected to a central computer then the system can be used to provide real-time frequency management of HF communications.

The definition of Sporadic E over a given area remains a more difficult problem. Measurements made by backscatter sounding in northern Australia indicate that when sporadic E is significant, the geographic area of coverage is often large (if variable in strength). This is one application where a backscatter sounder may provide the best solution (Houminer etal, 1996). Failing that, the highest possible density of reflection point coverage is needed and is most readily provided by networked oblique sounders.

In some parts of the world (notably Europe and some parts of the USA) the density of vertical ionosondes is such that an integrated system of vertical ionosondes alone would be sufficient to define the ionosphere over very large geographic areas if networking could be achieved. That would also appear to have been a possible goal arising from the PRIME project initiated by Peter Bradley. However on past performance, inter-country cooperation appears to be very difficult to achieve. For areas less well endowed, a network of combined vertical/oblique ionosondes will remain the most cost-effective solution. For ocean areas, the oblique sounding technique has no peer. Topside sounding provides an effective ionospheric slice along the satellite track as does tomography but neither can achieve a sufficiently high revisit rate without an increase in the number of relevant satellites.

References:

Clarke R.H., Fyfe D.F., Kettler D.I., Lynn K.J.W., Malcolm W.P., Sprey B.M., Taylor D.P. and Wright C.S., TENERP Conf. Proceedings, June 22-24, NPS, Monterey, CA., 1993.

Davies K., "Ionospheric Radio Propagation", NBS Monograph 80, 1965

Houminer Z., Russell C.J., Dyson P.L. & Bennett J.A., Ann.Geophys., V14, p1060, 1996.

Lynn K.J.W, World Data Centre Report UAG -104, p59, 1995.

Phanivong B, Chen, J., P.L. Dyson & Bennett J.A., J. Atmosp. Terr. Phys., V 57, p1715, 1995.

Poole A.W.V. & Mercer C.C., World Data Centre Report UAG -104, p59, 1995.

Samardjiev T, Bradley P.A., Cander L.R. & Dick M.I., PRIME COST 238 Workshop, p257, Graz, Austria, 1993.

8 DEPENDENCE OF THE DAYTIME foF2 VALUES IN THE POLAR IONOSPHERE ON THE MAGNETOPAUSE POSITION

L.N. Makarova and A.V. Shirochkov Arctic and Antarctic Research Institute 38 Bering Str., Saint-Petersburg, 199397 Russia

8.1 Introduction

The polar ionosphere is basically a part of the Earth's magnetosphere and therefore it is influenced the standard ionospheric controlling factors and also by the level of magnetospheric disturbance which, in its turn, is mainly controlled by the interplanetary magnetic field (IMF) and solar wind dynamics.

Among the IMF and solar wind parameters which can be considered as polar ionosphere controlling factors, the solar wind dynamic pressure Psw = mnV^2 (where m is a proton mass, n is the solar wind number density and V is the solar wind velocity) is a comparatively new candidate. Only recently Newell and Meng (1994) showed that enhanced solar wind dynamic pressure causes significant spatial changes to the particle precipitation regions of the magnetosphere. Contribution of other IMF and solar wind parameters to this process, including Bz, was rather insignificant.

Our straightforward attempts to find direct ionospheric signatures of the increased solar wind dynamic pressure give contradictory results. Sometimes notable drops in the daytime foF2 values at the high-latitude ionosondes, with a time lag of several hours, follow periods of enhanced Psw between the events. In these cases the diurnal variation of the F2 layer electron density actually disappears since the daytime and night-time foF2 values became equal. However, not every increase in Psw causes such dramatic ionospheric effects.

It is important to remember that the solar wind dynamic pressure is an external force determining the position of the Earth's magnetopause. The Earth's main internal magnetic field balances the solar wind dynamic pressure influence. The IMF is another force which influences the magnetopause position by means of geomagnetic field line erosion on the dayside of the magnetopause and by changing the net value of the Earth's magnetic field. Consequently it is necessary to take into account the influence of both the solar wind and the IMF to evaluate the magnetopause position. This has been done in the empirical model developed by Roelof and Sibeck [1993]. These considerations helped us solve the mysterious connection between the enhanced solar wind dynamic pressure and the previously mentioned anomalous foF2 diurnal variations. The former events occur only under a definite combination of IMF Bz-component and the solar wind dynamic pressure magnitudes, namely: when Bz is sufficiently negative and Psw is above about 2 hPa. Consequently it was quite naturally to try to find a connection between the daytime foF2 values in the polar ionosphere and the magnetopause position.

8.2 Results And Discussion

The ionospheric data used in this study were taken from the results of regular observations performed at several Russian ground-based vertical ionosondes: two Antarctic stations: Vostok (78.5 S;106.9 E; invariant latitude 83,2 S) and Mirny (66.6 S; 93.0 E; invariant latitude 76.9) as well as one Northern hemisphere station- Dixon (73,4 N; 80,6 E; invariant latitude 67.7 N). These stations were chosen for the study for two reasons: first of all, the very good quality of their data and second, to cover a wide range of invariant latitudes. Besides that, they represent both the Earth's hemispheres.

Noon (in magnetic local time - MLT) values of the F2 – region critical frequency – foF2 were taken, preferably during the winter season, in order to avoid periods when solar EUV radiation dominated the polar ionosphere. Statistically significant numbers of samples were taken to secure reliable results. Thus, data were taken for three winter months, day-by-day, apart from periods when IMF data were not available (King, 1977, 1986). The magnetopause position (in number of Earth radii – Re) was taken from the empirical model of Roelof and Sibeck (1993, their Figures 16 and 17) in accordance with the values of n, V and Bz, corresponding to the moment the foF2 recordings were made.

The results of this study are presented at Figure 1, where the foF2 noon dependence is given as a function of the subsolar magnetopause positions, expressed in the units of Re. The upper panel shows data for Vostok station, the middle one - for Mirny station while the bottom one - for Dixon. The results of a statistical analysis of the data are given on each

panel. One can see that the correlation coefficients, R, between the two sets of data are impressively high for all three stations, with a very high confidence level (p).

The general conclusion is that the daytime ionisation level in the polar ionosphere reduces to about half when the magnetopause approaches the Earth to a distance as close as about 9Re. It was shown earlier that for undisturbed conditions, the magnetopause is located at a distance of about 14Re [Holzer and Slavin, 1978]. The trend discovered seems to be universal, i.e it is common for the stations located in the polar cap, and in the auroral oval, of the both hemispheres. Another intriguing effect is evident at Figure 1. The slope of the linear regression lines changes with the invariant latitude of the observational point. It seems to be a signature of magnetopause shape changes near the Earth's geomagnetic pole.

Right now, little can be said about the exact physical mechanisms responsible for these phenomena whose reality is beyond any doubt. We are playing with an idea of the universal version of the global electric circuit with the magnetopause as the external element and the Earth's surface the internal one. In this scheme, inward and outward displacements of the magnetopause can be considered as a measure of energy accumulated in the "magnetosphere-ionosphere-atmosphere" system. Such an approach seems to have a good chance of explaining some existing puzzles. Our opinion is that solving these problems will shed new light on the whole fundamental problem of energy transfer from interplanetary space to the Earth's magnetosphere and ionosphere. The high degree of correlation between the daytime foF2 values in the polar ionosphere and the magnetopause position suggests a rough diagnostic for the latter parameter using standard ground-based vertical ionosonde data, i.e. to expand the possibilities for using these ionospheric observations.

8.3 Conclusion

A rather unexpected connection between the magnetopause position and the daytime ionisation level in the polar ionosphere is found. It is premature to present exact physical mechanisms responsible for this phenomenon. It must be done during future studies, but the results presented here are the good evidence of the hidden possibilities for standard, routine ionospheric observations whose value has sometimes been attacked by advocates of more sophisticated techniques.

References

R.E. Holzer and J.A. Slavin, Magnetic flux transfer associated with expansions and contractions of the dayside magnetosphere, J. Geophys. Res., 83 (A8), 3831-3840, 1978.

J.H. King, Interplanetary Medium Data Book, NASA, 1977,1986.

P.T. Newell and C.-I. Meng, Ionospheric projection of magnetospheric regions under low and high solar wind pressure conditions, J. Geophys. Res., 99 (A1), 273-279, 1994.

E.C. Roelof and D.G. Sibeck, Magnetopause shape as a bivariate function of interplanetary magnetic field Bz and solar wind dynamic pressure, J.Geophys.Res.,98 (A12),21421-21450,1993.

Figure 1. Dependence of the noon foF2 values recorded at three high-latitude stations Vostok (upper panel), Mirny (middle panel) and Dixon (bottom panel) on the magnetopause positions expressed in the Earth radius units. The wintertime foF2 data of the maximum solar activity epoch are presented. See the text for further explanations.

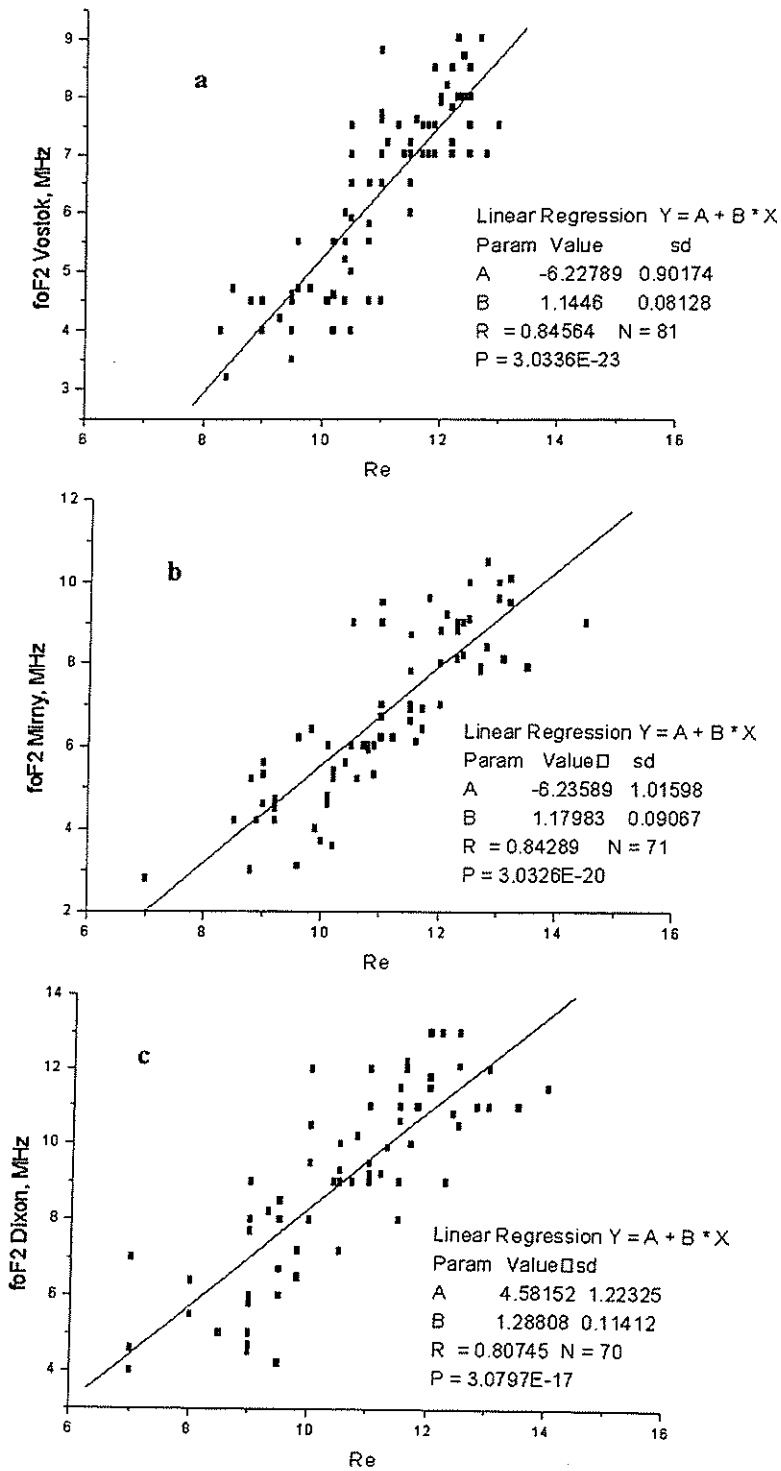

9 IONOSONDE ANTENNAS

Notes by J. W. Wright, Västervik Sweden

This article is an update on notes that were circulated to several people about two years ago.

Preliminary Comment: I am not an antenna expert and wish to avoid pretenses to that effect, but I have worked actively with a number of experts (mainly Dick Grubb, Walt Plywaski, Dick Kressman, and their own colleagues in this subject area) and I hope that what I have learned from them is not misrepresented here. I have tried to make some simple tests to reveal operational properties of antennas with which I have worked. These notes are intended to summarize these results for your information and critical comment. Some ideas for further work are included. *Note added 17 Oct 1997*: Having recently obtained some data from the San Diego dynasonde, I added its curve to Figure 5 together with a paragraph of discussion. For INAG, I have omitted personal names from the last section: 'Suggestions for Further Work' (you know who you are). Following the suggestions made, now two years ago when the document was distributed in hard copy to about 20 colleagues, no one has done anything except for some trials of the DATONG active antenna. I analyzed those results, with moderately discouraging conclusions, in a separate set of notes from which one paragraph is quoted later.

9.1 Introduction

In contrast to most other radars, the ionosonde is dependent on "echoes of opportunity" by critical reflection from ionospheric density contours; these are often tilted and irregular, much like an ocean surface. We desire broad antenna patterns, so as to sample as much of these structures as geometry and refraction will permit.

Ionosondes require antennas for transmission (Tx) and reception (Rx). Since spaced receiving arrays are essential for digital ionosondes, the question of using one and the same antenna for Tx and Rx does not arise (but such schemes are ill advised anyway, because of the nature of the MF/HF noise environment). The data to be shown here compare (at present) the *lumped* Tx, Rx performance of several systems. Since the available Tx choices differ more significantly than the Rx choices, we begin with a discussion of ionosonde transmitting antennas.

Difficulties arise in Tx design for vertical incidence ionospheric sounding in the MF/HF bands. The difficulties are greater for the digital research ionosondes of interest here, since we want quantifiable performance and must minimize two obvious, likely, and undesirable properties of simple antenna designs. With mention of their consequences for research ionosondes, they are:

a) Uneven radiation-pattern variations with frequency, which mask or bias ionospheric information bearing on

- field-aligned and field-normal scattering, as from plasma waves;
- auroral ion-cloud echolocations and E region lateral gradients;
- vector velocity estimation and derived electric fields, atmospheric gravity waves, winds and tides;
- dN/N estimation in Spread F; etc.

b) Uneven power-gain variations with frequency (in consequence of (a), or because of impedance mismatch, ground losses, etc.), which mask or bias ionospheric effects bearing on:

- non-deviative (D region) absorption and consequent N(h) inferences;
- deviative absorption near E region and F region penetrations, and consequent estimations of Te, Ti, υ_{ei}, υ_{en};
- discrimination among echoing processes: total internal reflection, Bragg and refractive scatter, etc.

Such measurements are the 'bread and butter' of the digital research ionosonde, and the choices of Tx and Rx are clearly critical to its success.

There are also some practical and engineering requirements that deserve attention:

c) The Tx must accommodate site constraints, aircraft (height) restrictions, climate hazards, and budget limits.

d) The Tx should minimize, and not provoke unnecessarily, RFI problems to civil and military telecommunications, nor to other experimental systems; in practice, this entails:

- Avoiding low angle radiation lobes, which are (usually) not useful for vertical sounding

anyway (but see comments in §2.5 on special applications for bistatic and 'auroral radar' measurements).

- Avoiding parasitic coupling to large vertical structures which will radiate vertical polarization; this argues against metallic support masts.

Additional considerations arise in considering the Rx options, of which the most important (not to be considered further here, however) is the need for accurate phase calibration.

9.2 Transmitter Options

There are two categories of practical Tx design: those characterized by a set of resonant (usually half-wave) lengths, and notional non-resonant structures. The latter (§2.1 and §2.2 below) manage to maintain some radiation at wavelengths small compared to the height and scale of the antenna ... but at the price of poor performance everywhere. They may be stabilized by a terminating resistor which consumes a significant part of the RF power.

The following are the Tx options known to me.

9.2.1 Vertical Delta

This is a cheap, dependable design, easy to erect on a single mast, long the standard for analog ionosondes at least in the USA program. I have used it (under protest) in an Equatorial dynasonde campaign, and therefore have some comparative data.

9.2.2 Vertical Rhombic

This is a classic design, often used for long haul broad band communications (then mounted more or less horizontally). I have no experience with this design. Mounted vertically, it might perform somewhat like the delta (which in fact is sometimes called a half-rhombic). It was long favored by German workers, and is still the choice of the Lowell digisonde group. It is suspended from a single mast. [A large example is installed with the digisonde at Ramfjordmoen, near the dynasonde's LPA, §2.5 below; this affords an excellent opportunity for objective comparisons].

9.2.3 Traveling-Wave Dipole

This requires two supporting masts of moderate height, perhaps more masts if made long enough to perform well below about 2 MHz. A quasi-resonant behavior is maintained by passive RC 'traps' at intervals within the dipole. It is used at USU's Bear Lake observatory and earlier, I believe, in their work at Siple Station Antarctica. I have very little experience with data from this antenna, but what I do have, is discussed below.

Log Periodic Antennas comprise a class which aims at frequency independence by the device of self-similarity in 'frequency periods' defined by a scaling factor $\tau < 1$. LPAs can be directed toward the ground, or upward. Provided the ground is electrically 'good', performance is generally better when the antenna is directed downward, so that each radiating element is at a constant height above its ground image, relative to its resonant length.

9.2.4 Single-Plane Log Periodic Dipole

This design resembles a plane triangle usually suspended between two masts. For the "Kinesonde in France" experiments, we used a single central mast instead, and declined the dipole elements toward ground at about 30 degrees below horizontal. We made extensive scale modeling and computer simulations, which suggested broad (roughly circular) patterns in both E and H planes, about 3 dB down at 60° zenith angle, and good frequency-independence within its 2 to 20 MHz design range. Below 2 MHz radiated power decreased smoothly at about 14 dB/octave. There was some evidence (in the scale model work) of self-interference toward the upper end of the frequency range. I do not have comparative data from this antenna at present, but the design is of some interest because commercial versions are available.

9.2.5 Two (or Four) Plane Wire Outline Trapezoidal Element LPA

This is the Tromsϕ antenna, with two planes. It is suspended from 4 masts at the corners of a square, within ropes that descend from the top of the masts to the center of the square at the ground. Two opposite, or all 4 triangular planes thus defined, may be filled with the zig-zag wire structure. We have some, but limited, experience with 4 plane structures. Except for certain special applications (see below), there seems to be no particular advantage to the 4-plane design. A detailed design drawing similar to the structure at Ramfjordmoen appears in Figure 1. This shows an antenna for the range 2.186 - 30.0 MHz with $\tau = 0.92$ suspended among masts of height 32m. (The Tromsø antenna, as built, may differ somewhat from these values). Unfortunately, figure 1 is the best small size figure that could be produced for publication. A larger, more readable version is available from the author for people seriously interested in constructing the antenna. For others, here is a description of the construction.

Figure 1: Log Periodic Antenna (LPA) similar to Tromso.

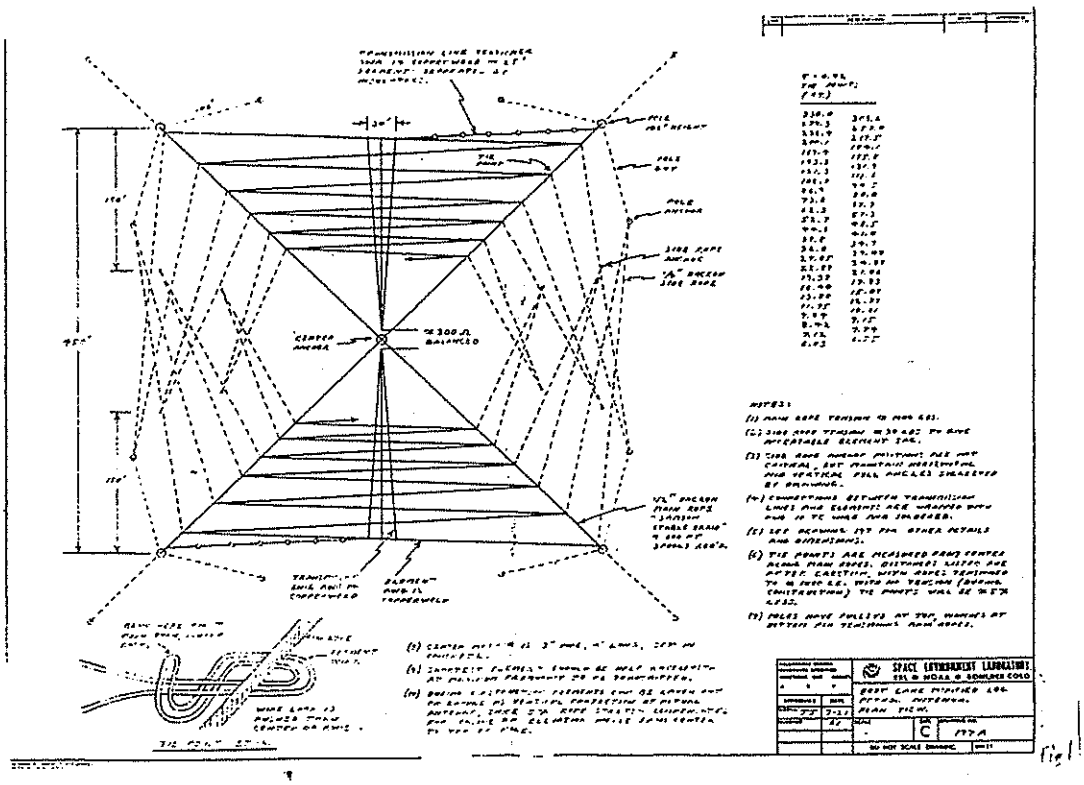

Figure 2. 243 UKDYNA 791541 echoes, May 1994. 1304 Jan 93 1,294623 echoes

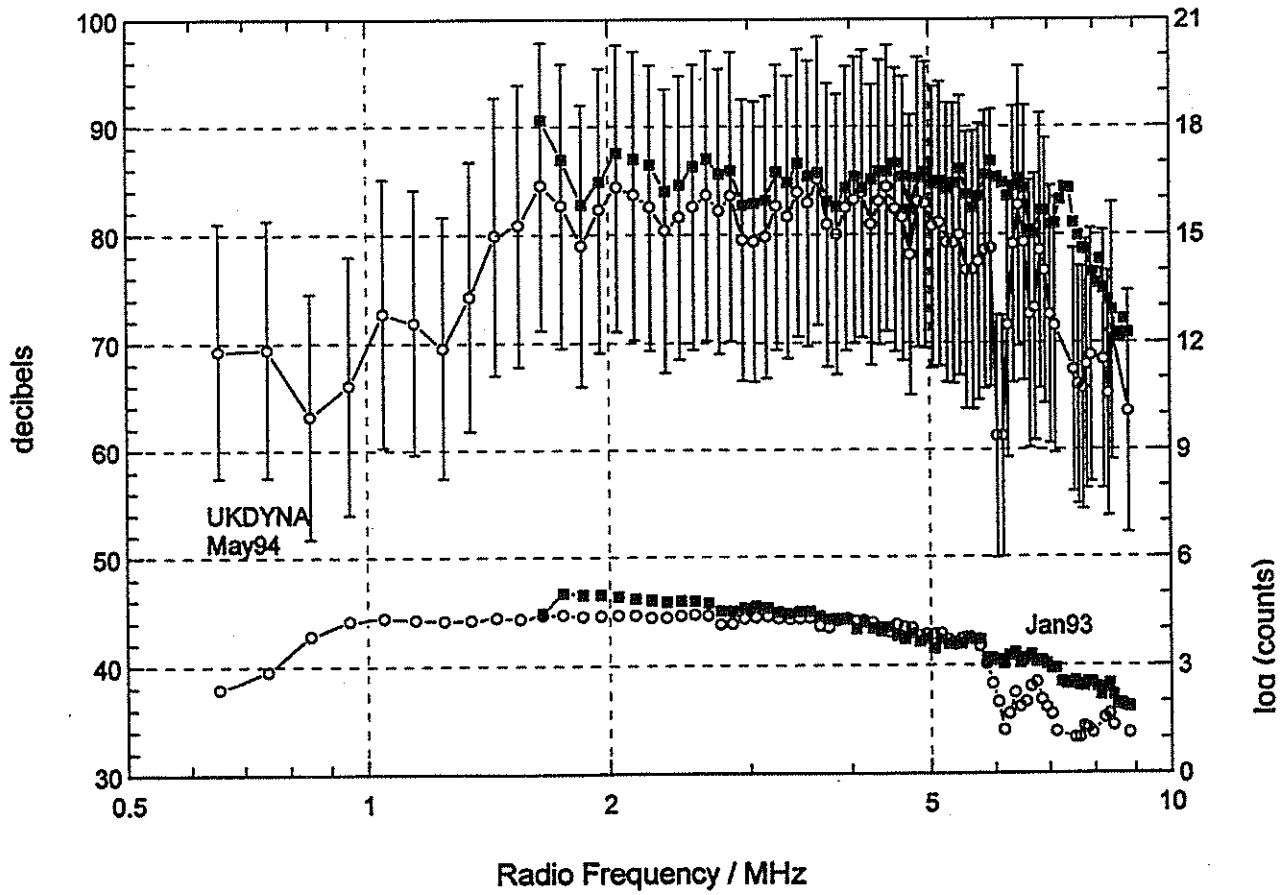

The antenna is strung on ropes attached (by pulleys for hoisting, repair and tensioning) to the tops of 4 poles 106' (21.3m) in height; the ropes meet at the center of the square defined by the poles, 450' (137.16m) on a side. Starting at two diagonally-opposite pole-top rope points, #14 AWG copperweld wire is punched through the ropes and wrapped tight. The wires then run in a clockwise direction to the next ropes to measured points, where a hairpin bend in the wires is again punched through the ropes and wrapped tight. The wires then run back again to the first ropes, zigzag fashion, and to the next (down) measured points. The measured points are expressed as the distance from the center vertex of this structure (near the ground) up along each rope. The first measured tie point (where the wires are first attached) is at 330.0' (100.58m) from the vertex. Subsequent tie points are at 0.92 of the preceding distance. For example, the 2nd tie points (on the other ropes clockwise), are at 303.6' (92.54m), and the 3rd tie points (back on the first ropes) are at 279.3' (85.13m). The whole thing is truncated at the 49th tie points at 6.03' (1.84m) on the first ropes, near where the zag length is half-wave at 25 or 30 MHz. We never use it up there.

In each of the two opposite tetrahedron faces thus filled by zigzags, a 3-wire feedline extends from near the ground out to the highest wires. The center wires of the feed lines go up the center to the center of the highest wires. The two other wires diverge linearly, to end at 15' (4.57m) each side of the center feed wire on the highest radiating wire. All wires are #14 copperweld. All 3 feed wires in each radiating plane are wrapped and soldered to the radiating wires where they cross.

The antenna is fed from a big 50-ohm coax line into a 50-ohm unbalanced-to-balanced 300-ohm transformer.

All of the distances cited are with the antenna tensioned (1000 lbs. in the diagonal ropes, plus some small tensioning ropes at the tie points). The ropes were chosen to have 5% maximum extension under tension.

The ground is *good* for RF, as far as I know, but there is no metallic ground plane. It is almost flat and horizontal, except for a 1.5m rise just outside the square on one side. If there is a standard way to quantify *good* or *fair* ground, it might be useful to compare with perfect ground, to learn what a metallic ground screen would accomplish.

The masts are the only expensive part of the construction. And metal masts, even if they are the most readily available and traditional for antenna work, are not really desirable: they tend to radiate parasitic energy, and they do so with vertical polarisation, the worst situation for RFI to nearby listeners. Also, they may damage the antenna performance. It needs to be modelled. A much better choice, if tall 'tree-masts' are unavailable or too expensive, are laminated wooden beams, as factory-made for auditorium rafters and similar applications. With (say) 25x25cm cross-section, and rope guys at top and mid-height; they serve very well (and have been in use at Tromsø for 17 years).

Another point to notice is that the antenna can be scaled to other low-frequency cuttoffs, which will change the required mast-height and ground area. The LPA might (with advance planning of its azimuth) serve for medium-distance oblique-incidence sounding between two similar ionosondes. For this purpose, one of the two radiating planes could be fed unbalanced to ground. This idea has not been modelled, and is conjectural; we will, however, do the modelling.

It is worth mentioning one option available with this design which to my knowledge has not been attempted, but which may well argue its consideration in certain situations (e.g., the prospective pair of dynasondes at Tromsø and Svalbard). For bistatic sounding between instruments spaced at distances of 500 to 1500 km, some power gain is necessary at the appropriate azimuth and zenith angle. Provided the LPA orientation is planned for this, a selected single plane of the structure may be driven *unbalanced* against ground to achieve this. The 4-plane structure provides, in addition to as many azimuth options, the feature that two planes might be reserved for vertical incidence work.

9.3 Rx Options

We can consider only Rx designs suitable in small arrays of 3 to 8 antennas within an area comparable to a favored radio wavelength, usually 100m or less. Radiation isolation between the antennas should be kept large, > 40 dB; this argues antennas small compared to their spacing. Four choices are currently of interest.

9.3.1 Small (30 MHz) passive dipoles

This was the choice advocated originally for the dynasonde. They are in use at the USU Bear Lake site, but were replaced at Tromsø in 1985 because of poor performance at frequencies below about 3 MHz.

Figure 3: 10 B and K-modes, USU Bear Lake TWD antenna; 21613 echoes

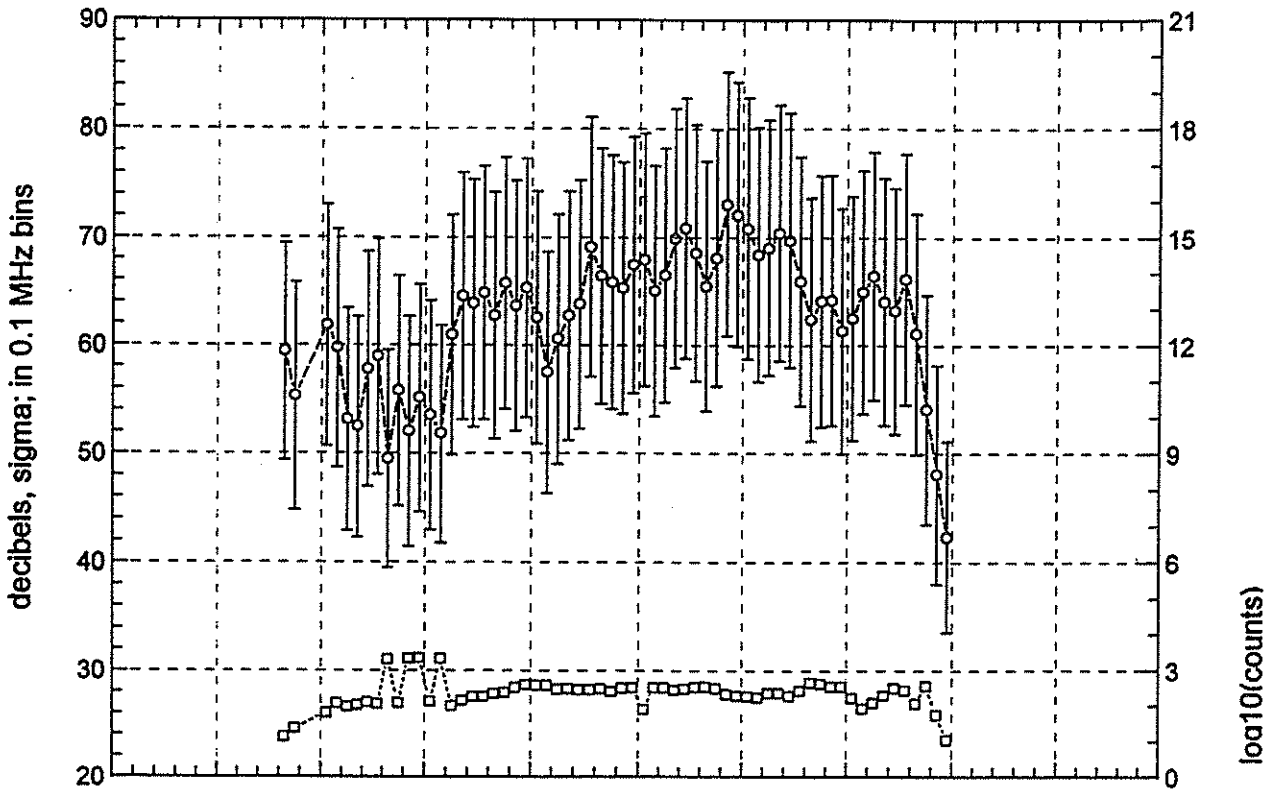

Figure 4: 44 Huancayo Z, K-modes; 121692 echoes. Simple delta antenna

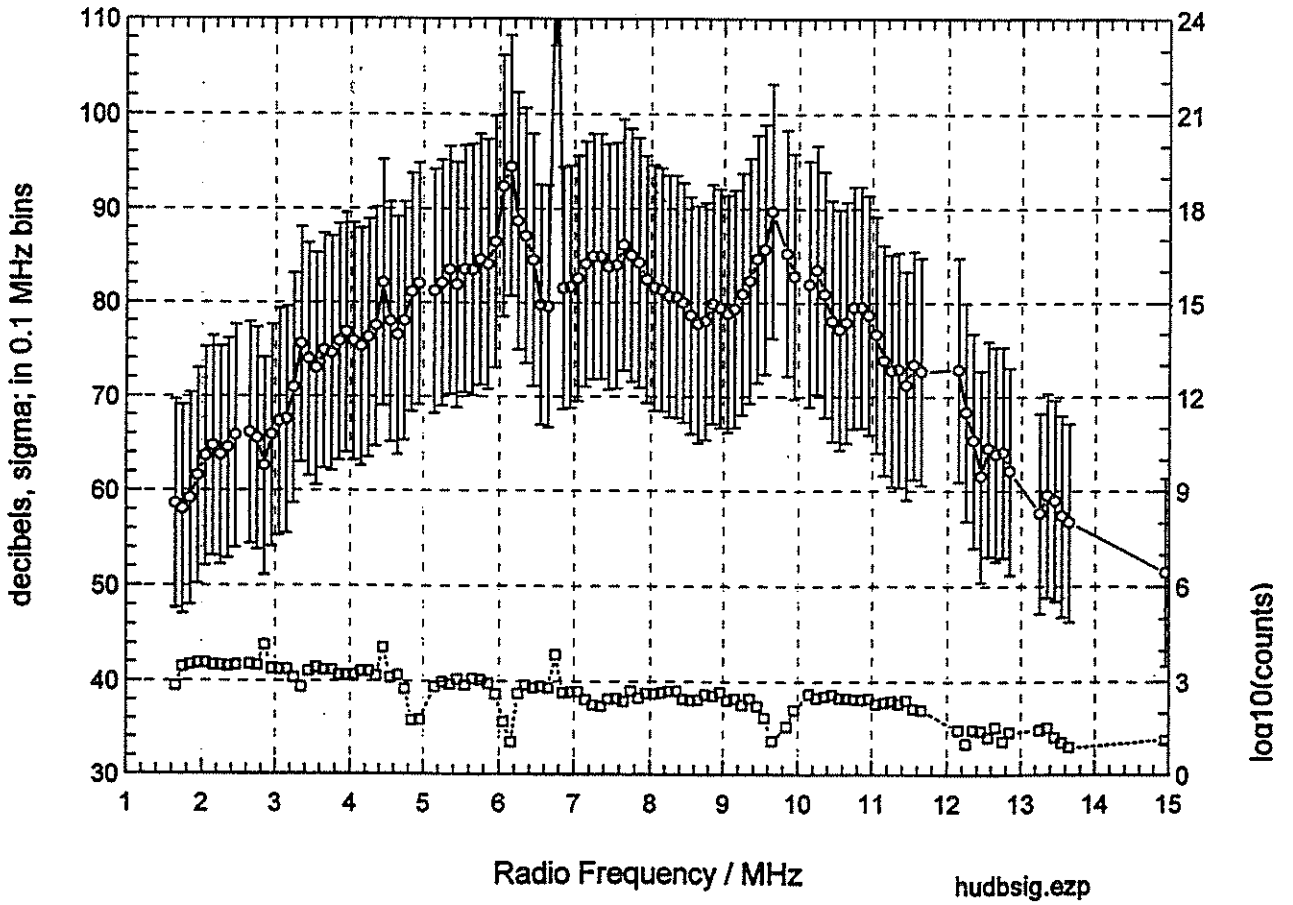

9.3.2 Small active dipoles

These have not yet been tried, but are of interest because one version is commercially available, and because they may overcome the limitations of the small passive dipole.

9.3.3 *Large* (6MHz) dipoles

These are used at Tromsø at present in a 'fat' version in which the elements are made of thick (15cm) tubing. Similar dipoles were used with the Huancayo dynasonde, but made of 5cm 'ladder wire'.

9.3.4 Small magnetic loops

These are favored by the Lowell Digisondes.

9.4 Overall Echo-Power Performances

We are in position to make some comparisons among the following antenna systems, in each case part of a NOAA dynasonde installation:

- Tromsϕ 2 plane, vertex down LPA, with 'fat' large receiving dipoles.
- Huancayo Delta, with ladder-wire large dipoles.
- USU Bear Lake TWD with small passive dipoles

Some idea of the performance of such systems, in the absence of absolute power and pattern calibrations, is given by analysis of ionospheric measurements made using them. I compare here some results using programs which read any number of ionosonde recordings, and which form the arithmetic means and standard deviations of selected echo variables in uniform (0.1 MHz) bins of radio frequency. Of particular interest, and generality, are the frequency profiles of echo-decibel powers, also further sorted by echolocations. Although a wide variety of natural processes affect these parameters, we can reasonably expect their large sample means to reveal some properties of the antenna systems in use. Of course, such results do not distinguish properties of the transmitting and receiving systems. The results also depend on the sample size, and (in part) on whether system calibrations exist. Comments about the role of such factors will be made in context.

Echo amplitude is computed as the arithmetic mean of the modulus of the complex amplitude components, among all receiving-antenna and deltaf 'channels' of a pulse set In our work at present, there are usually 8 such channels. For the work described here, the DSP system selects one complex amplitude for each channel nearest the mean echo peak. The linear amplitudes (A, initially expressed simply in ADC counts) are expanded according to the dynasonde decibel step attenuator ("AGC") settings, so that a very wide dynamic range is available in principle. The decibel power equivalent is $dB = 20\log_{10}(A)$. These steps are common to all of the data discussed here. However, a difference between the Huancayo data and the other examples must be noted. In the 1982 Huancayo case, the dynasonde-original ADCs were in use; a raw ADC count in the range ±2048 was a voltage in the range ± 8 volts. A recent hardware upgrade applicable to the Tromsϕ and USU Bear Lake data now expresses echo complex amplitude components in the range ± 5 volts. Thus 4.08 dB must be subtracted from the Huancayo decibel powers for comparison with the other data.

The 8 measuring channels are usually divided equally between the dynasonde's two 'identical' receivers, and often *un*equally among the several receiving antennas. Practices in this respect vary with the experiment, the experimenters' preferences, site constraints, etc. Although the individual receiving antennas could be studied, in the present work a single amplitude is first obtained as the average among the 8 channels.

To form the mean and standard deviation of echo decibel powers shown below, each echo was taken in sequence and assigned to its radio-frequency bin (0.1 MHz equal intervals). The mean and variance of the *linear amplitude* was up-dated in that bin by an algorithm designed for this purpose. The decibel equivalent of the mean and standard deviation were then obtained after all echoes were subsumed in this way. In another analysis routine, the echoes were further sorted into bins according to their zenith and azimuth angles of arrival. The mean, sigma variations of dB(f), without regard to echolocation, are shown first.

9.4.1 Tromsϕ LPA and fat dipoles (Fig. 2)

Figure 2 contains results from 243 B-mode recordings during the May 1994 UKDYNA campaign, and (analyzed separately) 1304 recordings from January 1993. Sigma 'error bars' are shown only for the May data. The two months differ significantly in solar illumination and consequent D-region absorption. Between 1.8 MHz and 5 MHz (May data), or up to 7 MHz (January data) the mean echo power is constant ± 2.5 dB, oscillating distinctly with a 'period' of 0.8. This oscillation is the log-periodicity designed into the antenna. The

apparent performance degradations above 5.5 MHz (May) and 7 MHz (January) may be identified with two causes:

(a) Insufficient sampling as the respective F-region penetration frequencies are reached. This is clear from the two lower curves, which show the (log) echo counts. Clearly, consistent mean powers and smooth frequency variations are obtained when a few100's of echoes are available in each bin; this condition is satisfied for all of the Jan93 bins (1,294,623 echoes subsumed, in all), but not uniformly so above 5.8 MHz in May94.

(b) Range dilation. Echo amplitude *A* decreases linearly with echo range; an echo from 600 km group range (R') suffers 15.6 dB more attenuation than an echo from 100 km for this reason. On average, above about 5.0 MHz in May, and above about 7 MHz in January, R' and dR'/df are large and increasing (with f).

Since fxF2 seldom exceeds about 8 MHz at Tromsø, it is difficult to appraise the system power performance at greater frequencies.

The January mean values exceed the May values by about 5 dB near 2 MHz, the difference decreasing to about zero by 5 MHz. This is qualitatively as expected by greater D-region absorption in May.

Below 1.8 MHz (May data only; a starting frequency of 1.7 MHz was used in January), the decibel amplitudes decrease by 18 dB per octave, as will be shown by a function (and its curve) later, in Figure 6. A decrement of 14 dB per octave below cutoff was obtained in modeling studies (1971) of the Log Periodic Dipole Antenna (§2.4). The decrement by the 2-plane antenna may well be less than that calculated for the LPDA, but the present data contain a contribution to this decrement from D-region absorption. The agreement with modeling therefore seems more than qualitatively satisfactory. It is also worth emphasizing that the LPA remains effective for data acquisition over a substantial frequency range below its design cutoff.

The decibel standard deviations are remarkably constant with frequency, about 12 dB, and as we shall see, they do not differ much among the other sites and antennas studied. The largest amplitude fluctuations are probably caused by geometric focusing (and, to a lesser extent, de-focusing) by ionospheric reflection-level curvatures, so it is not surprising that little variation of sigma occurs with frequency, antenna design, and observing site.

9.4.2 USU TWD Antenna and 30 MHz passive dipoles (Fig. 3)

This is a much smaller sample of data (10 recordings); below 2 MHz and above 7.8 MHz the dB variations are not meaningful for this reason. The effect of R' dilation above about 7.6 MHz is also evident. The 'spikes' of large count at 4 discrete frequencies near 3 MHz arises from the inclusion of two multi-fixed frequency "Kinesonde Mode" recordings in the sample. It may be noted that the mean, sigma in 3 of these frequency bins are not greatly different from their B-mode neighbors, by the factor 10 increase of echo count.

These are daytime recordings, and part of the general decrement of echo power with radio frequency < 5 MHz is the result of D-region absorption. However, the irregular fluctuations with frequency, and in particular the odd behavior near 3 MHz, are likely to be characteristic of the antenna system. I do not know the radio frequencies corresponding to the resonant LC traps in the TWD, so cannot associate them with features in the figure.

9.4.3 Huancayo Delta Antenna and ladder wire long dipoles (Fig. 4)

Over most of the graph, the data count is adequate to define the mean and sigma. The recordings span the transition from day to night, so D-region absorption again contributes to the decreasing power below, say, 6 MHz. However, the broad scale shape of the curve is probably characteristic of the Delta antenna. Isolated peak counts near 2.9, 4.5 and 6.8 MHz result from multi-fixed-frequency recordings in K-mode. Count minima at 4.8, 6.15 and 9.7 MHz are harder to explain. The latter two minima are associated with wider decibel peaks, but no decibel feature is seen at 4.8 MHz. We shall see below that an explanation is perhaps found in the antenna radiation pattern.

The dimensions of this "small delta" are not definitely known to me, but a characteristic scale is probably about 25m in height and base length; if 50m approximates its natural "resonance" wavelength, (although the delta is intended *not* to be a resonant structure), this may explain its general peak of performance near 6 MHz, as well as the sharp peak near there.

9.4.4 Comparison of the 3 systems (Fig. 5)

Recall from the discussion above, that 4.08 dB should be subtracted from the entire Huancayo graph of Figure 4, for consistency with Figures 2 and 3.

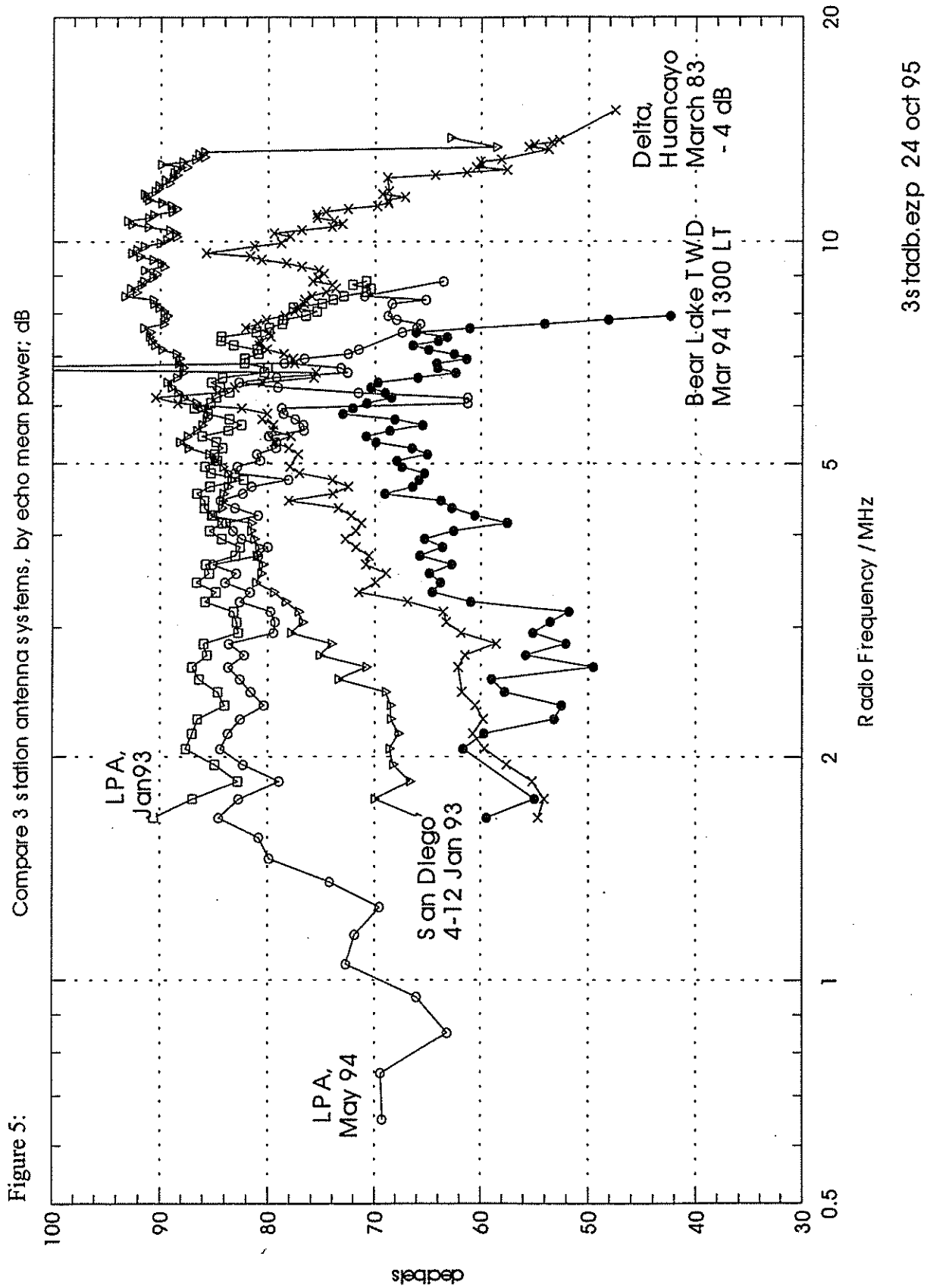
Compare 3 station antenna systems, by echo mean power; dB
3stadb.ezp 24 oct 95
Radio Frequency / MHz
decibels
100
90
80
70
60
50
40
30
0.5
1
2
5
10
20
LPA,
Jan93
LPA,
May 94
San Diego
4-12 Jan 93
Bear Lake T W D
Mar 94 1300 LT
Delta,
Huancayo
March 83
- 4 dB

Figure 5:

This comparison is made explicit in Figure 5, where all 3 systems are represented on the same decibel scale and without their sigma data. Since the transmitter power is about equal among these systems, and the receiving antennas at Tromsø and Huancayo are fairly similar, the LPA *vs* Delta comparison is more or less direct. However, a further 3 dB might be subtracted from the Huancayo curve since that system was laid out so as to put all of the radiated energy into the (equatorial linear) O-mode polarization. The other systems enable O and X (circular) polarizations, and the power is divided about equally between them.

To compare the USU system with the others, we need some idea of the role played by the 30 MHz receiving dipoles at Bear Lake. In July 1985, while similar 30 MHz receiving dipoles were still in service at Tromsø, a prototype of the present fat dipole was constructed. Here are the decibel differences for the same ionospheric echoes received by each type:

Tromsø receiving antenna comparison, 19 July 1985

Radio Frequency	0.7	1.0	1.6	2.0	2.6	3.0	3.6	4.6	MHz
FatD-30MHz dipole	15	13	10	10	10	10	10	10	dB

With these points in mind, we may conclude from Figure 5 that the TWD performs somewhat better (in terms of received echo power only) than the Delta near and below 2 MHz, but both are at least 15 dB inferior to the LPA. The TWD and Delta then become roughly comparable toward higher frequencies, although the TWD is less smooth. By about 6 MHz, all three antennas provide comparable echo power.

There are too few echoes at Tromsø and Bear Lake at higher frequencies to permit good comparisons. However, because of its self-similarity up through 20 MHz, there are few reasons to expect that the LPA performance changes markedly, whereas the Delta almost surely continues the declining performance already evident above 10 MHz. If the Delta were made larger to improve its performance at low frequencies, the high-frequency rolloff would commence proportionately lower too. Presumably, the bandwidth of the TWD can be extended upward with additional LC traps, but perhaps at the price of further degradation of its performance at low frequencies.

9.4.5 San Diego Dynasonde (Fig. 5 – continued)

Figure 5 now (Oct 1997) includes results from the San Diego dynasonde. Unfortunately, I do not know the details of its Tx antenna, but it was probably a delta built to larger scale than the Huancayo delta. The curve is about 10 dB above the Huancayo curve, which can probably be attributed in part to the San Diego receiving antennas: they were "fat dipoles" built to conform rather closely to the Tromso Rx antennas. The table above compares these dipoles to the USU–type short dipoles, not to the ladder wire Huancayo dipoles of length similar to Tromso and San Diego. It is very likely that if a delta was used, it included 'broadbanding' improvements (a diverging 3–wire structure) which were not used at Huancayo. These factors probably account for the 10 dB difference. The San Diego curve includes many more ionograms that for Huancayo, accounting for its smoother variation.

9.5 Radiation-Pattern Performance

Results in the preceding paragraphs are "all-sky" averages. It is of interest to know how these systems differ in their spatial directivity. Where we see variations of performance with radio frequency, it is possible that variations of radiation pattern are occurring as well. The desired information is therefore three-dimensional (decibel dependence on azimuth sector (AZ), zenith zone (ZN) and radio frequency, f), which considerably aggravates the problems of binning sufficient data and of graphical representation. (Actually, the methods used here do not require large-memory arrays, and the concise results can be up-dated with new data as they become available, utterly without limit. But the methods are at present 'data-starved').

Instead of pursuing the full 3-dimensional problem, I have therefore elected to bin and display two 2-dimensional representations: AZ(f), averaged over all zenith angles; and ZN(f), averaged over all azimuths. The "SKYSORT" analysis routine permits choice of the bin resolution in each dimension. It would be desirable to use at least 8 azimuth sectors, and perhaps the same number of zenith zones. There are not enough data (except at Tromsø) to support this at present, so for the sake of uniformity just 4 AZ sectors (90°) and 6 ZN zones (10°, all echoes

>60° lumped into the outer zone) have been specified for each site. The *count* of echoes occurring in each bin is subject to a number of geophysical factors (differing among the 3 sites presently available), in addition to antenna effects, but in most cases the geophysical effects should have little influence on the mean echo power.

9.5.1 Tromsϕ LPA and fat dipoles, (Figs. 6 (AZ) and 7 (ZN))

Only the May 1994 data were analyzed for the present purpose; the January 1993 data (included in Figures 2, 5) were obtained using only 4 of the available 6 antennas at Tromsø, and as a result they suffer excessive echolocation aliasing. In Figure 6 the mean dB(f) is shown for the four cardinal azimuth sectors, superimposed. Except at a few frequencies, there is no significant dependence on azimuth. There is a substantial dependence on zenith angle, as shown in Figure 7. The log-periodicity of the LPA remains evident in both figures, and there is no evident tendency for the curves to converge or diverge in concert with the ± 2.5 dB oscillation identified with this design parameter.

The zenith-angle variation is fairly well described by a $\cos^{12}$ (ZN) law (e.g., -8 dB at 30°, -14 dB at 40°): a $\cos^3$ amplitude law is often assumed for a horizontal dipole near ground, so $\cos^6$ applies to power, and this is squared again if both Tx and Rx behave as dipoles.

The dynasonde receiving array at Tromsø is very near the eastern edge of a large 2.75 MHz dipole array of the 'PRE' experiment; in fact, the dynasonde 'W' antenna is literally beneath the outer dipole elements of PRE. (This very undesirable situation is a result of crowded antenna siting constraints there). The effect of this arrangement is not known a-priori, but we have found in other work that echo amplitudes from the W antenna are lower, and some phase shift is introduced near 2.75 MHz. It is likely that features in Figures 6, 7 between 2 and 3 MHz give further evidence of these coupling effects.

It should be noted that even the most extreme zenith angles (i.e., ≥ 60°) are represented in Figure 7, throughout the frequency range. Some workers might question the usefulness of this broad skyview; I am confident, however, that this is a useful feature: the most compelling reason arises in the estimation of vector velocities, where the horizontal components must be determined by their projection on the line-of-sight Doppler measurement. The more remote echoes contribute the most definitive information in this way.

Although the point is peripheral to our present purpose, it is also worth noting that the lowest amplitudes in Figure 7 are systematically at the largest zenith angles. This is quite compelling evidence that the 6ANT array scheme, together with the full 'UNIPHASE' analysis developed for it, accomplishes its intended echolocation anti-aliasing purpose. As mentioned above, I could not use the large Jan93 database for this analysis because only the outer 4 antennas of the 6ANT array were used in that campaign. When the present SKYSORT analysis *is* nevertheless applied to this dataset, very characteristic and systematic aliasing effects are immediately apparent. More specifically, out of the 1.31×10^6 echoes, *none* are observed at a limiting zenith angle ZNL, which increases systematically with radio frequency:

SKYSORT with 15 zenith zone bins; Tromsø 4ANT, January 1993

ZNL		6	12	18	24	30	36	42	48	degrees
radio freq.		1.95	2.15	2.35	2.65	3.15	3.75	4.95	6.95	MHz

This means that, for a given zenith angle ZN > ZNL, all such echoes alias into a smaller ZN. It also means that at any radio frequency > 1.95 MHz using 4ANT, there is a substantial risk (increasing with frequency) that any chosen echo may have returned from a larger zenith angle than the value estimated.

There are other aliasing risks to consider, and 6ANT is not free of them; nor is it completely free of echolocation aliasing at the highest frequencies. New work on these questions is underway.

The results of the present section, together with those of §4.1, show that the Tromsø antenna system performs rather faithfully in accord with LPA and dipole theory (apart from the PRE effects). The results suggest that an absolute calibration of the system power (permitting corrections to individual data for Tx rolloff <1.8 MHz, for the ±2.5 dB log-periodic factor, and for the $\cos^{12}$ (ZN) law) may

Figure 6: 243 UKDYNA 791541 echoes, May 1994. 4 Azimuth Sectors

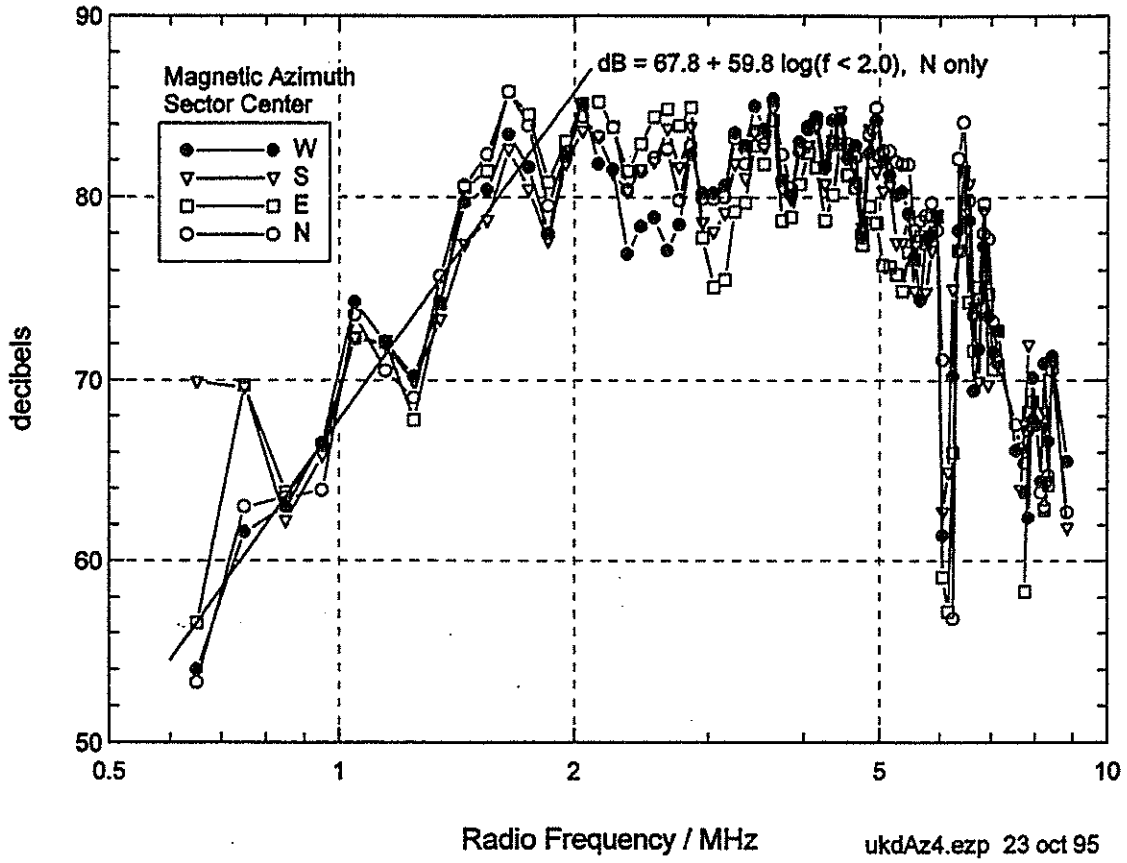

Figure 7: 243 UKDYNA 791541 echoes, May 1994. 6 Zenith Zones

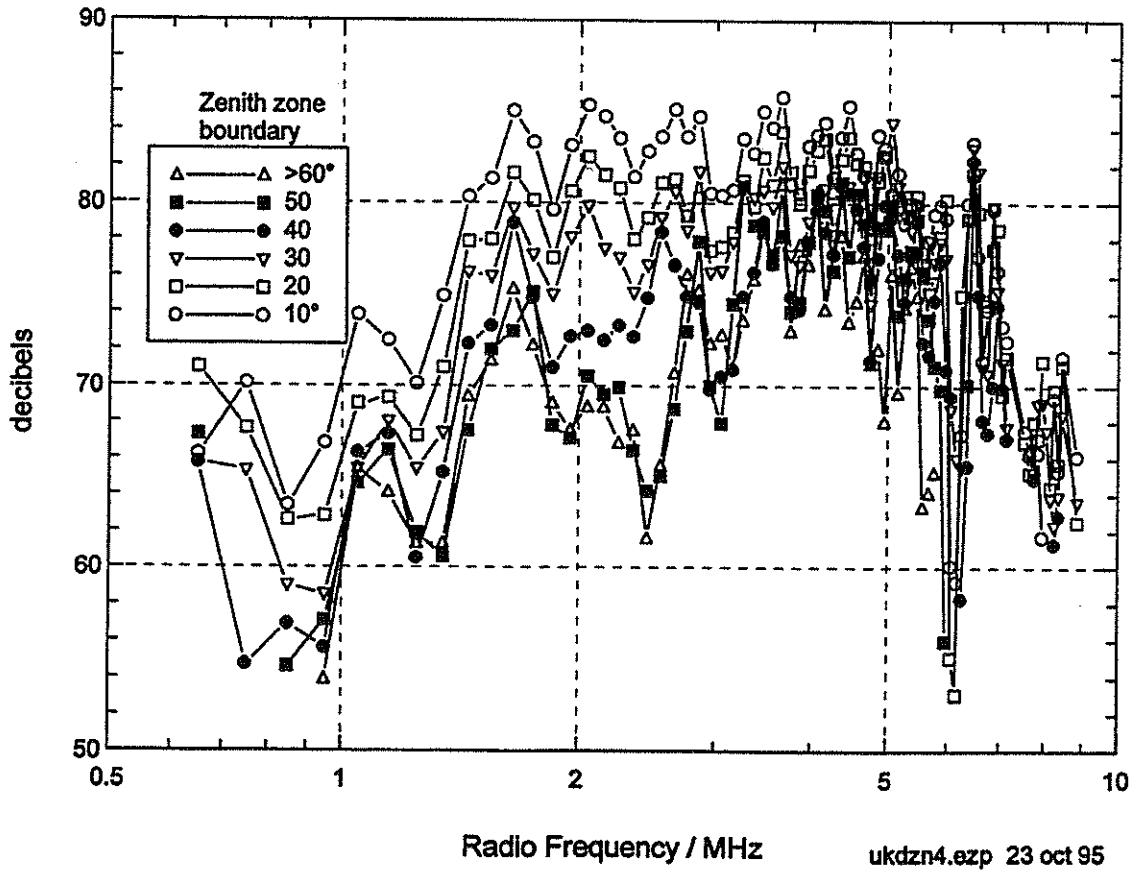

Figure 8: 10 B and K-modes, USU Bear Lake TWD antenna; 21613 echoes

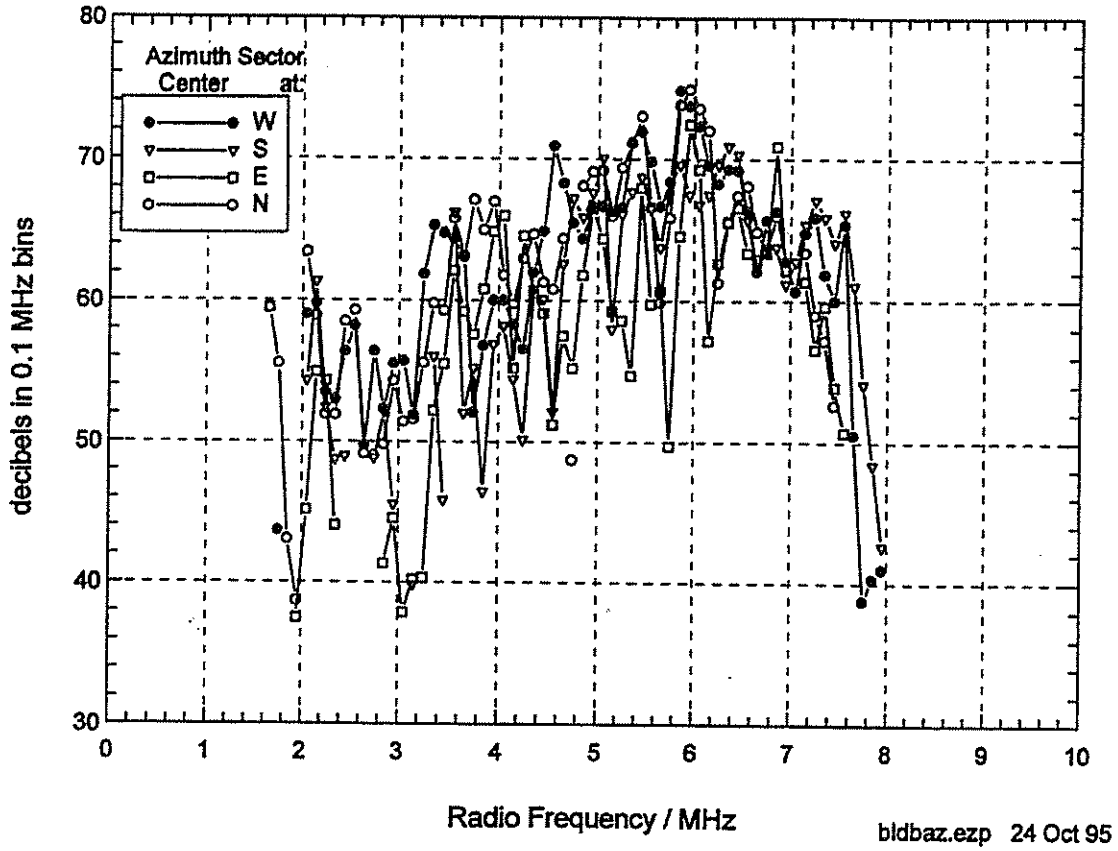

Figure 9: 10 B and K-modes, USU Bear Lake TWD antenna; 21613 echoes

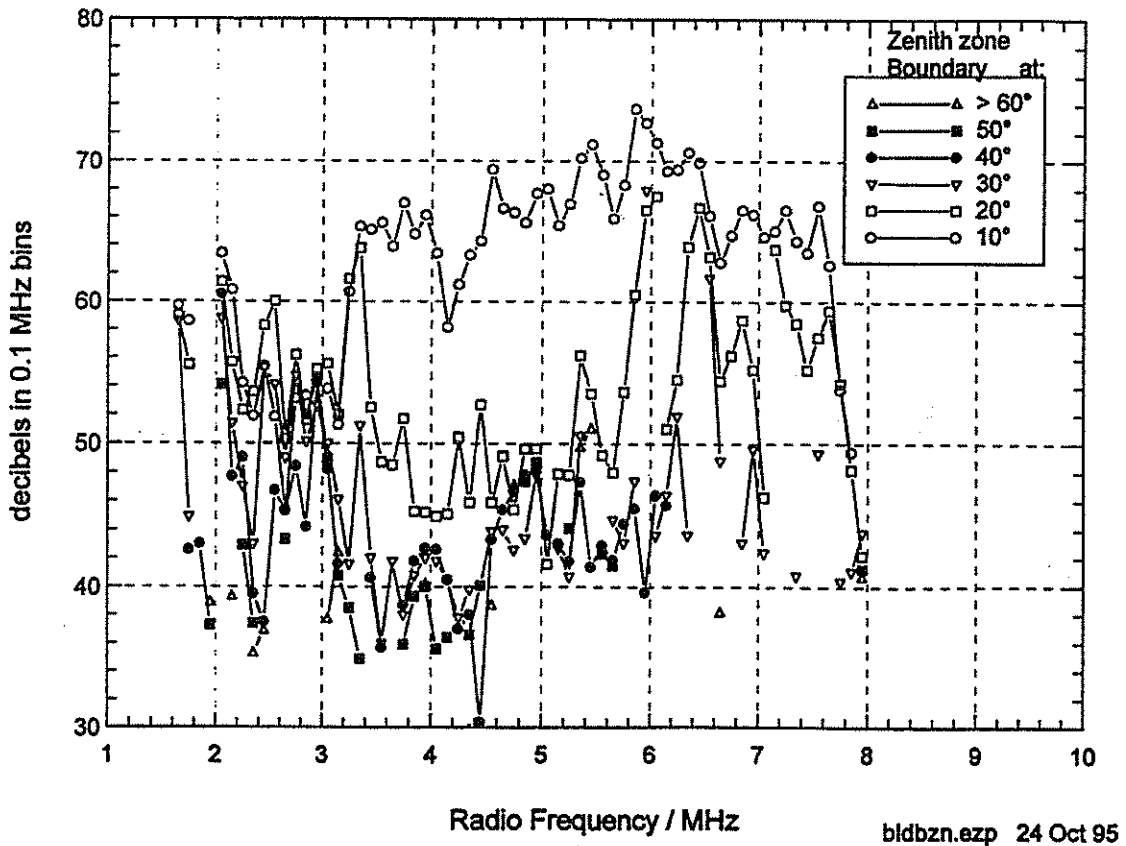

Figure 10: 44 Huancayo Z, K modes; 121692 echoes.

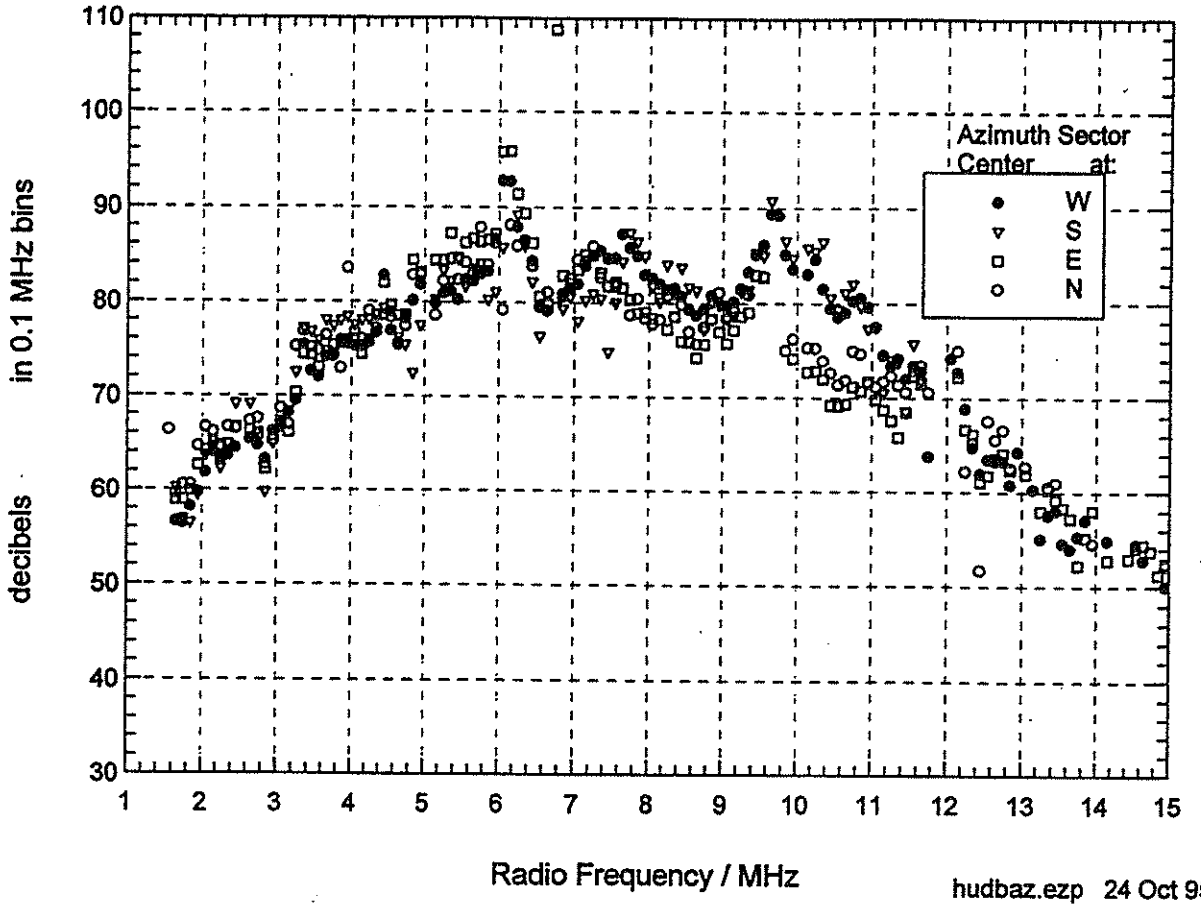

Figure 11: 44 Huancayo Z, K modes; 121692 echoes.

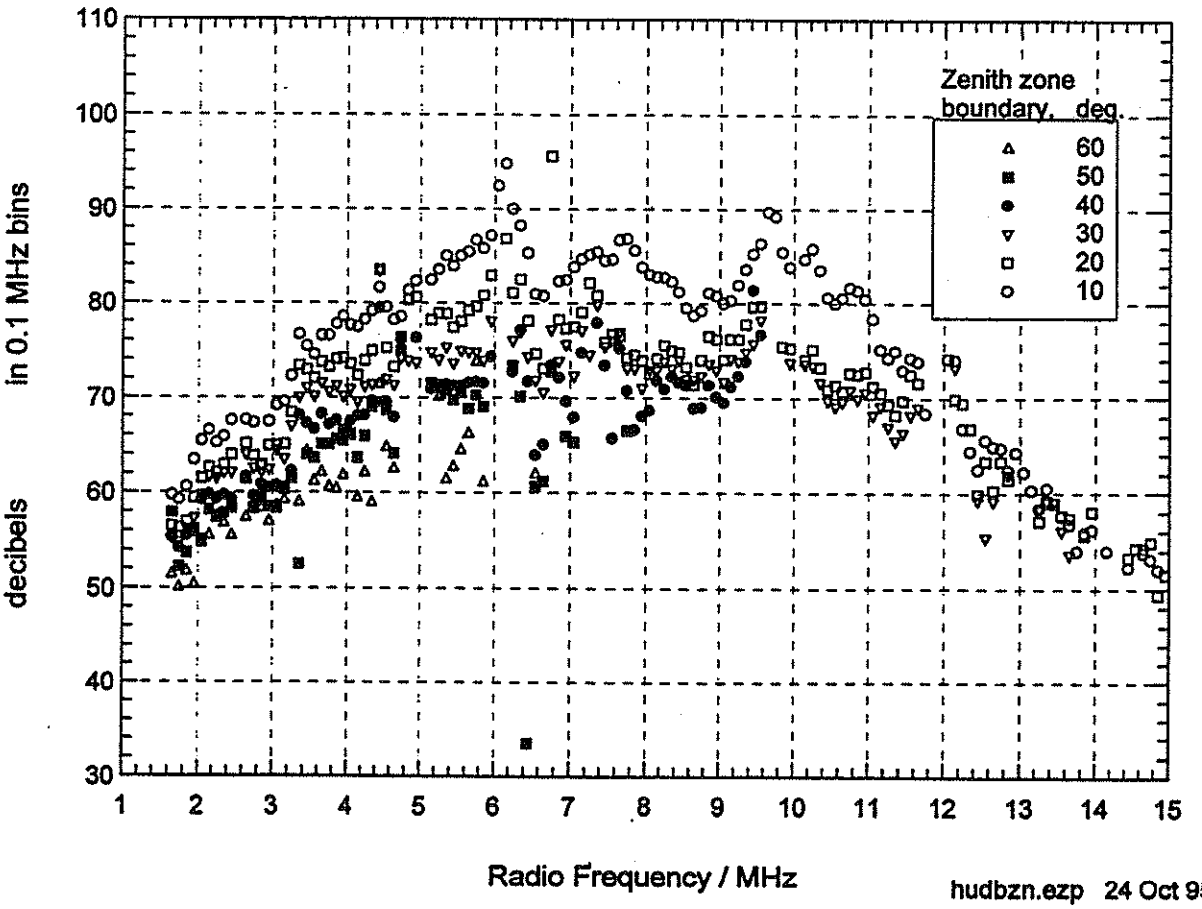

be within reach. I believe that the results also justify taking the Tromso system as a 'benchmark' for comparison with the other two systems available at present; this tone which will be perceived in the remainder of these notes.

USU TWD Antenna and passive 30 MHz dipoles, (Figures 8 (AZ) and 9 (ZN))

There is a tendency, although not at all frequencies, for stronger echoes to return from the West and North in Figure 8. The antenna system is laid out on a hillside (orientation?), which might account for this effect. There are perhaps too few echoes per f, AZ bin to be confident of any conclusions, but there seems to be some evidence of southward 'lobeing' (periodic minima). The decibel range and variability with azimuth is certainly larger than for the LPA.

The zenith-angle results, Figure 9, suggest that the system changes 'character' at 3 MHz and again at 6 MHz. Between these limits, the zenith (10°) zone returns echoes some 15 dB stronger than those from the outer zones, even from the 20° zone; this seems to argue a very directive antenna system in this range. With their Rx baseline (D = 30m), the USU receiving array cannot alias echolocations below 5 MHz. Even at 7 MHz, aliasing is only possible beyond $\sin^{-1}(\lambda/2D) = 46°$, so this is not likely to account for the observations.

9.5.2 Huancayo Delta Antenna and ladder wire long dipoles, (Figs. 10 and 11.)

Here we encounter important physical effects which may bias the echolocations. The nearly horizontal magnetic field (dip -0.5°), together with field-alignment of most irregularities, reduces the count of echoes from the N/S plane, except from near the zenith (as an aspect of measurement noise, if nothing else). This probably accounts for much of the tight clustering without regard to azimuth in figure 10. There is, however, consistent evidence for stronger echoes from W than from E, above about 7 MHz. This is perhaps a natural (plasma-wave, or 'equatorial bubble') scattering effect.

The same D = 30m as at USU was used here, but a so-called 'NOPOL' Rx scheme (all antennas pointing northward) effectively doubled the smallest possible aliasing angle frequency, to 10 MHz. There is, accordingly, progressive absence of larger zenith angles with frequency > 10 MHz in Figure 11. Allowing for this, the decibel spread between small and large zenith angles increases fairly rapidly and steadily with frequency in Figure 11, although the power is always largest from the zenith. The implication is clearly of a broad polar diagram (comparable to the LPA or dipole) at low frequencies (< 3 MHz), becoming much more narrow at high frequencies.

9.6 Suggestions for Further Work

I realize that this topic is not exciting physics, but I think it may well be material to doing good physics with digital ionosondes. I would therefore like to see it pushed further. Simply getting a bigger database for the sites studied here is both possible and desirable. Adding sites, especially where they involve different antenna choices, different ionospheric (and ground) conditions, etc., will help clarify the whole picture and permit more objective choices in establishing new sites or upgrading existing ones. I wish to end these notes with some specific suggestions. I will be grateful for comments, corrections and suggestions. Where more data analysis is indicated, I shall be happy to undertake it, provided I can receive the data (and read it !), on floppy, CD-ROM, QIC-80 tape, or by ftp. Alternatively, I can provide copies of the two short Fortran subroutines that produced the results discussed here.

9.6.1 Similar, or further, analyses from dynasonde sites.

NOAA Boot Lake, Colo.	LPA, small dipoles, good ground
EISCAT, Tromsø	LPA, fat dipoles fair ground
Halley Bay; BAS	LPD, small dipoles, no ground
USU Bear Lake;)	TWD, small dipoles
Los Alamos; Huancayo	LPA, fat dipoles, poor ground

9.6.2 Similar analyses from digisondes

University of Tromsø	Immense Rhombic; mag. loops
La Trobe University	Small Rhombic? mag. loops?
RAL, UK	ditto ?
Anywhere	any other ?

9.6.3 Similar analyses from other digital ionosondes

Canadian digital ionosonde	?
Are there others ?	?

9.6.4 Some unique questions awaiting answers or work at Tromsø

- Compare the (digisonde) mag loop Rx with (dynasonde) fat dipoles: simply run a cable to the nearest one, and patch it into an unused MUX port temporarily. Just a few such recordings, comparing the *same echoes*, should tell the tale, regarding echo power *vs* frequency.
- Is an effective off-vertical lobe generated by one plane of the Tromsø LPA, when it is driven unbalanced to ground, and does the transmitter complain? What matching transformer is needed? Try it; compare forward/reflected power too.
- Compare the DATONG active small dipole with fat dipoles and with passive small dipoles; same procedure as above; *however*:
- Is the DATONG antenna likely to have wild, unpredictable or large phase vs frequency behavior? To learn this, we need a spaced pair or some enlightened comment.
- Will the DATONG perform better over an artificial (chicken wire) ground plane
- How much better? How big must such a ground plane be, to be useful (i.e., the whole Rx array? Just a few meters^2). Try it and see.
- How do the DATONG antennas perform as a crossed pair (i.e., with more or less mutual coupling than the fat dipoles)?

[Note added, 7 Nov 1997: Some tests were done of two DATONG active antennas at Tromsø. They were not sufficiently extensive to answer all of the questions above, but they do suggest that the DATONG is not the active antenna of choice for improving ionosonde data. Here is a paragraph quoted from my notes of 14 March 1996:

"We could almost certainly NOT simply exchange the existing NESWes 6ANT dipoles for Datongs, without unacceptable penalties in lost or weak echoes and poorer S/N. On the other hand, they are probably much better at low frequencies than the non-active short dipoles (such as at Bear Lake). So a comparison with those would still be informative".]

10 "CHARS" : URSI IIWG Format For Archiving Monthly Ionospheric Characteristics

Bodo W. Reinisch, Center for Atmospheric Research, University of Massachusetts, 600 Suffolk Street, Lowell, MA 01854, USA
Bodo_Reinisch@uml.edu, http://ulcar.uml.edu

10.1 Introduction

The format "CHARS" is now used by the World Data Centers (WDC) for archiving monthly ionospheric characteristics; it was first introduced in 1989 by Gamache and Reinisch [1989a]. The CHARS "database" is actually a collection of the flat ASCII files each storing a month of data. This design was essentially an inexpensive way to provide potential users of the data with a platform-independent access to the CHARS database contents. The FORTRAN source code for reading the CHARS files has been released in a Scientific Report [*Gamache and Reinisch*, 1994]. The software for automatic assembly_of CHARS files from the individual ionogram SAO files (see SAO Document in this INAG Newsletter) is currently under development.

The Ionospheric Informatics Working Group (IIWG) of URSI Commission G had recommended the CHARS format as a standard for scaled ionogram data dissemination and archival in 1989. This format was then accepted as the URSI standard at the URSI General Assembly in Prague, 1990. This report, prepared with the help of Ivan Galkin, Xueqin Huang and Jim Scali, presents the general description of the CHARS format with the latest updates as of November 1997. A description of the CHARS document is also contained on our web site. Comments on improvements, errors, or inconsistencies should be sent to the University of Massachusetts Lowell.

10.2 CHARS Format for Ionospheric Characteristics

The CHARS file is a flat ASCII text file containing all available data for a month, including the time series of major characteristics and their hourly statistical features (medians, deciles, etc.) It is reasonable to expect that the sounding schedule would not be strictly regular within the observation month. To solve a problem of uneven time sampling, a special header record is introduced into CHAR files [*Gamache and Reinisch,* 1989b] to serve as a key to encoding/decoding the remainder of the file.

Historically, the maximum length of individual text lines in a CHARS file was set to 120 characters so that it still could be printed without wrapping. The number of lines in a file is determined by the number of days in the month, the number of measurements made each day, and the number of characteristics being archived.

The structure of the CHARS file is shown in Table 1. It consists of two headers, **Station Header** and **Data Header**, followed by the main **Data Group**.

10.3 Station Header

The Station Header is one line comprising informative and encoding data. It contains the **Station Name** and location *(A30)* format; the **Station Code** in *(A5)* format; the **meridian time** used by the station to indicate if time is recorded in UT or LT on the records is given next in *(I4)* format followed by the station coordinates, **Latitude N** and **Longitude E** both in *(F5.1)* format; next there are two *(A10)* format variables describing the **Scaling type**, this takes the value *Manual* or *Automatic*, and the **Data editing** variable which can be *Edited*, *Non-Edited*, or *Mixed.*; last in this line is space for the **Ionosonde system name** in *(A30)* format. Total length of the Station Header is 99 characters plus CR and LF.

10.4 Data Header

Data Header contains information necessary to properly arrange and represent the Data Group. It starts with the **Year**, **Month**, **Number of days** in the month, **M**; the **Number of characteristics** archived in the CHARS file, **K**; the **Total number of measurements** reported for the CHARS file, and the **Number of daily measurements** made for each of the **M** days. Two lines of integers in (30I4) format are required to store this part.

Then, a repeating format of *(12A10)* is used to list the **Names** of the particular characteristics being archived. There is **K** of them, hence more than one line might be required to fit all names. For example if only the critical frequencies were archived, foF2, foF1, and foE, **K** would be three, and the characteristics list would be ' foF2' ' foF1' ' foE'. A list of the names of the characteristics, the

units, and URSI codes taken from UAG23 [*Piggott and Rawer*, 1978] are given in Table 2. The URSI list has been expanded with characteristics that are scaled by the Digisonde ARTIST [*Reinisch and Huang, 1983; Tang et al.* 1989]. The Chebyshev coefficients [*Huang and Reinisch*, 1996] used to represent the electron density profiles are also given, also the best B0 and B1 parameters [*Reinisch and Huang, 1997*] for the IRI F2-profile, and the calculated ionospheric electron content.

Next, the **Units** corresponding to the characteristics list (see Table 2) are given in the file, these are in *(12A10)* repeating format. The last lines of the Data Header are for the **URSI codes** specified for each of the characteristics (see Table 2) and written in *(60A2)* repeating format.

From the information in this Data Header one knows immediately how many data for the time or for each characteristic are to be read. From the number of measurements for each day the time data can be separated into the times for the individual days of the month and the measured characteristics can uniquely be associated with a given time on a given day.

Finally, the Data Header contains the measurement times for the month. With uneven time spacing the measurement times must be recorded to associate with the reported characteristics. This requires that hours, minutes, and seconds of each measurement be entered into the database. To conserve space, the times are written once per month and the reported characteristics are written to correspond to these times. The measurement times are written in a *(30(3I2))* repeating format corresponding to the **hours**, **minutes**, and **seconds**, HHMMSS, of the measurements. The number of lines needed for this is determined by the data sampling rate for the month.

10.5 Data Group

The Data Group contains the actual values of the characteristics and the corresponding hourly medians and statistics. The group is comprised of a number of lines per each archived characteristic which are repeated for each characteristic. The order of the characteristics follows that given in the "List of characteristics". On a per characteristic basis, for each characteristic one has the N_1 values of the characteristic for day 1 corresponding to the reported measurement times for day 1. These are followed by the values for day 2, day 3, ... for each of the **M** days of the month. The characteristics are written in a repeating *(24(I3,2A1))* format corresponding to the integer value (I3) of the characteristic and the qualifying and descriptive letters [see UAG 23]. The actual values of the characteristics can be obtained by multiplying the integer value by the value found in the corresponding Units list (group 2) of the database record (see Table 2). Thus a value of 86 reported for foF2 is multiplied by the Units factor 0.1 MHz to give a foF2 value of 8.6 MHz.

The IIWG Workshop 1989 suggested the use of two slashes, //, in place of the qualifying and descriptive letters for monthly characteristics data that were autoscaled but not validated or "edited", i.e. where no quality control procedure has been applied. This code has been extended to consider data that have been edited but no descriptive or qualifying letters introduced. With two positions to fill and the use of a single or double slash there are four codes that can be defined. The first is no slashes implying the use of the descriptive or qualifying letters. The next is the use of two slashes which signifies no editing and no intended use of des/qual letters. The third choice is to put a slash in the first position followed by a blank. This is used to signify autoscaled data that have been edited but no descriptive or qualifying letters are used. The last possibility is a blank in the first position followed by the slash. This is not currently used thus it leaves the possibility for future extension of the code. The codes are summarized in Table 3.

Immediately following the characteristics data are the **hourly medians** given in a *(24(I3,2A1))* format; the **counts** for the hourly medians and the **range** in *(24(I2,I3))* format; the **upper quartiles** in a *(24(I3,2A1))* format; the **lower quartiles** in a *(24(I3,2A1))* format; then the **upper deciles** in a *(24(I3,2A1))* format; and finally the **lower quartiles** again in a *(24(I3,2A1))* format.

The above sections are repeated for each characteristic given in the "characteristics list." This completes the CHARS file, i.e. a month of characteristics data.

10.6 References

Gamache R. R. and B. W. Reinisch, Proceedings from the International Workshop on "Digital Ionogram Data Formats for World Data Center Archiving," University of Lowell Center for Atmospheric Research, November 1989a.

Gamache R. R. and B. W. Reinisch, Ionogram Characteristics at Uneven Data Rates, Presented at *URSI Working Group G.4 Ionospheric Informatics International Workshop*, July, 1989, University of Lowell Center for Atmospheric Research, 1989b

Gamache R. R. and B. W. Reinisch, Ionospheric Characteristics Data Format for Archiving at the World Data Centers, *University of Lowell Center for Atmospheric Research, Sci.Report 467*, 1994.

Huang X. and B.W.Reinisch, Vertical .Electron density profiles from the Digisonde network, Adv. Space Res. **6**, *121-129*, 1996

B.W. Reinisch and X. Huang, Automatic Calculation of Electron Density Profiles from Digital Ionograms. 3. Processing of bottomside ionograms*Radio Science*, **18**, *477-492* 1983

Reinisch, B. W. and X. Huang, Fitting the IRI F2-profile function to measured bottomside profiles, Adv. Space Res., in print, 1997

Piggott W. R. and K. Rawer, Editors, *U.R.S.I. Handbook of Ionogram Interpretation and Reduction*, World Data Center A for Solar-Terrestrial Physics Report UAG-23, and 23A, Boulder CO (1978).

Tang J., R. R. Gamache, and B. W. Reinisch, Progress on ARTIST Improvements, *Sci. Report No. 14, GL-TR-89-0185*, 1989.

Table 1. IIWG CHARS File Structure for Flexible Data Rates

File Section	FORTRAN Format	Description
Station Header	A30	Station Name
	A5	Station code
	I4	Meridian time used by station on records
	F5.1	Latitude N
	F5.1	Longitude E
	A10	Scaling type: Manual/Automatic
	A10	Data editing: Edited/Non-edited/Mixed
	A30	Ionosonde system name
Data Header	30I4... *1	Year
		Month
		Number of days in the month, **M**
		Number of Characteristics, **K**
		Numbers of measurements total
		Numbers of measurements for each of the **M** days ($\mathbf{N_i}$, i=1..**M**)
	12A10...*	Names
	12A10...*	Units
	12A10...*	List of corresponding URSI codes
	20(3I2)...*	Measurement times HH:MM:SS for each of **M** days, $\mathbf{N_i}$ values
Data Group	24(I3,2A1)...*	$\mathbf{N_1}$ values of characteristic 1 (Day 1)
		$\mathbf{N_2}$ values of characteristic 1 (Day 2)
		$\mathbf{N_M}$ values of characteristic 1 (Day M)
	24(I3,2A1)	24 hourly medians for characteristic 1
	24(I2,I3)	24 x 2 hourly counts and ranges
	24(I3,2A1)	24 hourly upper quartiles
	24(I3,2A1)	24 hourly lower quartiles
	24(I3,2A1)	24 hourly upper deciles
	24(I3,2A1)	24 hourly lower deciles
		Repeated for characteristic 2
	...	
		Repeated for characteristic **K**

1* The format is repeated for as many lines as needed to store the data

Table 2. List of Characteristics, URSI codes, and Units

Group	CHARACTERISTIC				Units	UAG23	DEFINITION
	ARTIST		URSI				
	Name	#	Name	#		ref. #	
F2		1	foF2	**00**	0.1 MHz	1.11	The ordinary wave critical frequency of the highest stratification in the F region
			fxF2	**01**	0.1 MHz	1.11	The extraordinary wave critical frequency
			fzF2	**02**	0.1 MHz	1.11	The z-mode wave critical frequency
	M(D)	3	M3000F2	**03**	.01	1.50	The maximum usable frequency at a defined distance divided by the critical frequency of that layer
	hpF2	12	h'F2	**04**	km	1.33	The minimum virtual height of the ordinary wave trace for the highest stable stratification in the F region
			hpF2	**05**	km	1.41	The virtual height of the ordinary wave mode at the frequency given by 0.834 of foF2 (or other 7.34)
			h'Ox	**06**	km	1.39	The virtual height of the x trace at foF2
	MUF(D)	4	MUF 3000F2	**07**	0.1 MHz	1.5C	The standard transmission curve for 3000 km
			hc	**08**	km	1.42	The height of the maximum obtained by fitting a theoretical h'F curve for the parabola of best fit to the observed ordinary wave trace near foF2 and correcting for underlying ionization
			qc	**09**	km	7.34	Scale height
F1		2	foF1	**10**	.01 MHz	1.13	The ordinary wave F1 critical frequency
			fxF1	**11**	.01 MHz	1.13	The extraordinary wave F1 critical frequency
				12			not used
			M3000F1	**13**	.01 MHz	1.50	See Code 03
			h'F1	**14**	km	1.30	The minimum virtual height of reflection at a point where the trace is horizontal
				15			not used
	hpF	11	h'F	**16**	km	1.32	The minimum virtual height of the ordinary wave trace taken as a whole
			MUF 3000F1	**17**	0.1 MHz	1.5C	See Code 07
				18			not used
				19			not used
E		9	foE	**20**	.01 MHz	1.14	The ordinary wave critical frequency of the lowest thick layer which causes a discontinuity
				21			not used
			foE2	**22**	.01 MHz	1.16	The critical frequency of an occulting thick layer which sometimes appears between the normal E and F1 layers
			foEa	**23**	.01 MHz		The critical frequency of night time auroral E layer
	hpE	13	h'E	**24**	km	1.34	The minimum virtual height of the normal E layer trace
				25			not used
E2			h'E2	**26**	km	1.36	The minimum virtual height of the E2 layer trace
Auroral E			h'Ea	**27**	km		The minimum virtual height of the night time auroral E layer trace
				28			not used

Table 2. List of Characteristics, URSI codes, and Units (continued)

Group	CHARACTERISTIC				Units	UAG23 ref. #	DEFINITION
	ARTIST		URSI				
	Name	#	Name	#			
				29			not used
Es layer		6	foEs	**30**	0.1 MHz	1.17	The highest ordinary wave frequency at which a mainly continuous Es trace is observed
			fxEs	**31**	0.1 MHz	1.17	The highest extraordinary wave frequency at which a mainly continuous Es trace is observed
		47	fbEs	**32**	0.1 MHz	1.18	The blanketing frequency of the Es layer
			ftEs	**33**	0.1 MHz		Top frequency Es any mode.
	HpEs	14	h'Es	**34**	km	1.35	The minimum height of the trace used to give foEs
				35			not used
			Type Es	**36**		7.26	A characterization of the shape of the Es trace
				37			not used
				38			not used
				39			not used
Other 1			foF1.5	**40**	.01 MHz	1.12	The ordinary wave critical frequency of the intermediate stratification between F1 and F2
				41			not used
		5	fmin	**42**	0.1 MHz	1.19	lowest frequency at which echo traces are observed on the ionogram
			M3000 F1.5	**43**	.01 MHz	1.50	See Code O3
			h'F1.5	**44**	km	1.38	The minimum virtual height of the ordinary wave trace between foF1 and foF1.5 (equals h'F2 7.34)
				45			not used
				46			not used
			fm2	**47**	0.1 MHz	1.14	The minimum frequency of the second order trace
			hm	**48**	km	7.34	The height of the maximum density of the F2 layer calculated by the Titheridge method
			fm3	**49**	0.1 MHz	1.25	The minimum frequency of the third order trace
Spread F Oblique			foI	**50**	0.1 MHz	1.26	top ordinary wave frequency of spread F traces
		10	fxI	**51**	0.1 MHz	1.21	top frequency of spread F traces
			fmI	**52**	0.1 MHz	1.23	lowest frequency of spread F traces
			M3000I	**53**	.01 MHz	1.50	See Code 03
			h'I	**54**	km	1.37	The minimum slant range of the spread F traces
			foP	**55**	0.1 MHz		Highest ordinary wave critical frequency of F region patch trace
			h'P	**56**	km		Minimum virtual height of the trace used to determine foP
			dfs	**57**	0.1 MHz	1.22	The frequency spread of the scatter pattern
				58		7.34	Frequency range of spread fxI-foF2
				59			not used

Table 2. List of Characteristics, URSI codes, and Units (continued)

Group	CHARACTERISTIC				Units	UAG23 ref. #	DEFINITION
	ARTIST		URSI				
	Name	#	Name	#			
N(h) Titheridge method		30	fh'F2	**60**	0.1 MHz	7.34	The frequency at which h'F2 is measured
		29	fh'F	**61**	0.1 MHz	7.34	Frequency at which h'F is measured
				62			not used
			h'mF1	**63**	km	7.34	maximum virtual height in the o-mode F1 cusp
			h1	**64**	km	7.34	True height at f1 Titheridge method
			h2	**65**	km	7.34	True height at f2 Titheridge method
			h3	**66**	km	7.34	True height at f3 Titheridge method
			h4	**67**	km	7.34	True height at f4 Titheridge method
			h5	**68**	km	7.34	True height at f5 Titheridge method
			H	**69**	km	7.34	Effective scale height at hmF2 Titheridge method
T.E.C.			I2000	**70**	10^{16} m^{-2}	7.34	Ionospheric electron content Faraday technique
			I	**71**	10^{16} m^{-2}	7.34	Total electron content to geostationary satellite
		39	I1000	**72**	10^{16} m^{-2}	7.34	Ionospheric electron content to height 1000 km using Digisonde technique
				73			not used
				74			not used
				75			not used
				76			not used
				77			not used
				78			not used
			T	**79**	10^{16} m^{-2}	7.34	Total sub-peak content Titheridge method
Other 2		7	FMINF	**80**	0.1 MHz		Minimum frequency of F trace (50 kHz increments) Equals fbEs when E present
		8	FMINE	**81**	0.1 MHz		Minimum frequency of E trace (50 kHz increments).
		15	HOM	**82**	km		Parabolic E layer peak height
		16	yE	**83**	km		Parabolic E layer semi-thickness
		17	QF	**84**	km		Average range spread of F trace
		18	QE	**85**	km		Average range spread of E trace
		22	FF	**86**	.01 MHz		Frequency spread between fxF2 and fxI
		23	FE	**87**	.01 MHz		As FF but considered beyond foE
		25	FMUF 3000	**88**	.01 MHz		MUF(D)/obliquity factor
		26	h'MUF 3000	**89**	km		Virtual height at fMUF
N(h)		15	zmE	**90**	km		Peak height E layer
		33	zmF1	**91**	km		Peak height F1 layer
		32	zmF2	**92**	km		Peak height F2 layer
		34	zhalfNm	**93**	km		True height at half peak electron density
		37	yF2	**94**	km		Parabolic F2 layer semi-thickness
		38	yF1	**95**	km		Parabolic F1 layer semi-thickness
				96			not used
				97			not used
				98			not used
				99			not used

Table 2. List of Characteristics, URSI codes, and Units (continued)

Group	CHARACTERISTIC				Units	UAG23 ref. #	DEFINITION
	ARTIST		URSI				
	Name	#	Name	#			
Digisonde Profile, F2 layer			[A_0F2]	**A0**	km		Coefficient A_0, truncated to integer km
			<A_0F2>	**A1**	m		A_0 - [A_0], truncation remainder
			[A_1F2]	**A2**	km		Coefficient A_1, truncated
			<A_1F2>	**A3**	m		A_1 - [A_1]
			[A_2F2]	**A4**	km		Coefficient A_2, truncated
			<A_2F2>	**A5**	m		A_2 - [A_2]
			[A_3F2]	**A6**	km		Coefficient A_3, truncated
			<A_3F2>	**A7**	m		A_3 - [A_3]
			[A_4F2]	**A8**	km		Coefficient A_4, truncated
			<A_4F2>	**A9**	m		A_4 - [A_4]
			[fsF2]	**AA**	MHz		starting frequency, truncated
			<fsF2>	**AB**	kHz		fs - [fs]
			[fmF2]	**AC**	MHz		ending frequency, truncated
			<fmF2>	**AD**	kHz		fm - [fm]
			[hmF2]	**AE**	km		peak height, truncated
			<hmF2>	**AF**	m		hm - [hm]
			ε_{pp}F2	**AG**	0.1 km		error per point, an average mismatch of original h'(f) trace and the trace reconstructed from the calculated profile
Digisonde Profile, F1 layer			[A_0F1]	**B0**	km		Coefficient A_0, truncated to integer km
			<A_0F1>	**B1**	m		A_0 - [A_0], truncation remainder
			[A_1F1]	**B2**	km		Coefficient A_1
			<A_1F1>	**B3**	m		A_1 - [A_1]
			[A_2F1]	**B4**	km		Coefficient A_2
			<A_2F1>	**B5**	m		A_2 - [A_2]
Digisonde Profile, F1 layer continued			[A_3F1]	**B6**	km		Coefficient A_3
			<A_3F1>	**B7**	m		A_3 - [A_3]
			[A_4F1]	**B8**	km		Coefficient A_4
			<A_4F1>	**B9**	m		A_4 - [A_4]
			[fsF1]	**BA**	MHz		starting frequency of the layer, truncate
			<fsF1>	**BB**	kHz		fs - [fs]
			[fmF1]	**BC**	MHz		ending frequency fm
			<fmF1>	**BD**	kHz		fm - [fm]
			[hmF1]	**BE**	km		peak height
			<hmF1>	**BF**	m		hm - [hm]
			ε_{pp}F1	**BG**	0.1 km		error per point, an average mismatch of original h'(f) trace and the trace reconstructed from the calculated profile

Table 2. List of Characteristics, URSI codes, and Units (continued)

Group	CHARACTERISTIC				Units	UAG23 ref. #	DEFINITION
	ARTIST		URSI				
	Name	#	Name	#			
Digisonde Profile, E layer			[A_0E]	**C0**	km		Coefficient A_0, truncated to integer km
			<A_0E>	**C1**	m		A_0 - [A_0], truncation remainder
			[A_1E]	**C2**	km		Coefficient A_1
			<A_1E>	**C3**	m		A_1 - [A_1]
			[A_2E]	**C4**	km		Coefficient A_2
			<A_2E>	**C5**	m		A_2 - [A_2]
			[W]	**C6**	km		Valley width [W], truncated
			<W>	**C7**	m		W - [W]
			[D]	**C8**	km		Valley depth [D], truncated
			<D>	**C9**	m		D - [D]
			[fsE]	**CA**	MHz		starting frequency
			<fsE>	**CB**	kHz		fs - [fs]
			[fmE]	**CC**	MHz		ending frequency "
Digisonde Profile, E layer			<fmE>	**CD**	kHz		fm - [fm]
			[hmE]	**CE**	km		peak height "
			<hmE>	**CF**	m		hm - [hm]
			ε_{pp}E	**CG**	0.1 km		error per point, an average mismatch of original h'(f) trace and the trace reconstructed from the calculated profile
IRI			ValleyID	**CH**			Valley Model ID=400 for NHPC4.00
			B0	**D0**	km		IRI Thickness parameter
			B1	**D1**	0.1		IRI Profile Shape parameter
				D2			not used
				D3			not used
				D4			not used
				D5			not used
				D6			not used
				D7			not used
				D8			not used
				D9			not used

10.7 Table 3. IIWG Codes for the Descriptive and Qualifying Fields of the Characteristics.

Symbolic code	Description
Q D	Qualifying and descriptive letters used according to UAG #23A.
/	Data, edited but no qualifying and descriptive letters used.
_ /	No current meaning, for future extension.
/ /	Autoscaled data, no editing, no qualifying and descriptive letters used.

11 SAO (STANDARD ADEP OUTPUT): FORMAT FOR IONOGRAM SCALED DATA ARCHIVING

Bodo W. Reinisch, Center for Atmospheric Research, University of Massachusetts, 600 Suffolk Street, Lowell, MA 1854, USA
E-mail: Bodo_Reinisch@uml.edu; http://ulcar.uml.edu

11.1 Introduction

Automatic scaling of ionogram data has come a long way and the quality of the autoscaled data has reached a remarkable level. Consequently the time has arrived to directly transfer ionosonde data to the World Data Centers using the Internet. We have begun to equip the Digisondes with Internet connections. The first Internet links were established between the Okinawa Digisonde (CRL, Japan) and the WDC-C2 in Tokyo, the Millstone Hill Digisonde (UML, USA) and the WDC-A in Boulder, Colorado, and the Chilton Digisonde (RAL, GB) and the WDC-C1 in Chilton. All data generated in the Digisonde are made available for electronic transfer: ionogram data, scaled data, and drift data.

Starting in 1987, the Ionospheric Informatics Working Group (IIWG) of Commission G of URSI has developed recommendations for the data formats to be used for dissemination and archiving of scaled ionogram data and for the monthly ionospheric characteristics. The IIWG abstained (wisely) from trying to develop a common data format for the system-dependent ionogram and drift data.

The following report gives a description of the Standard ADEP Output (SAO) format as of November 1997 and was prepared with the help of Ivan Galkin, Jim Scali, Xueqin Huang and Bob Gamache. Each SAO (text) file contains the scaled data for one ionogram including the echo traces h'(f), echo amplitudes, frequency and range spread, etc. and the electron density profile [Huang and Reinisch, 1996]. The new SAO files also contain a listing of the N(h) profiles, and the IRI profile parameters B0 and B1 [Reinisch and Huang, 1997]. The upgraded or new Digisondes [Reinisch et al., 1997] produce the SAO files in real time for local recording and/or electronic transfer. The older Digisondes generated only binary files that do not contain all the characteristics listed below. The SAO file structure has remained the same since its development by the IIWG in 1989, but the content has been expanded. Since these Digisonde-ionogram SAO files are now becoming available to many user either through the WDC's or via the web pages for the connected Digisonde sites it seems important to publish a description of the SAO format. We make reference to our homepage for a more complete report: http://ulcar.ulm.edu. The structure of these SAO files is such that it can be used for scaled ionogram data from any ionosonde and it was the recommendation of the URSI Working Group that this file structure be used for the exchange of scaled ionogram data.

A document on the updated version of the Monthly Characteristics File structure (CHARS) is presented in this INAG Newsletter.

11.2 Standard ADEP Output "SAO" Format

The SAO format was originally designed to store output records produced by an ADEP program developed by UMLCAR for editing the results of automatic scaling. The format was first presented at an International Workshop on Digital Ionogram Data Formats for the World Data Centers in Lowell in 1989 [*Gamache and Reinisch,* 1989] and recommended as an international standard for archiving ionogram data. The following is a description of the SAO format version 4.0 [*Gamache et al.*, 1996].

An SAO file is an ASCII text file with a maximum line length of 120 characters. In order to describe the database concisely some definitions are necessary. The nomenclature is as follows:

File:	collection of many Records
Record:	all data for a single measurement
Group:	all Lines of a datum type
Line:	a sequence of Elements of a datum type, CR/LF terminated
Elements:	a single datum in the specified format.

The *Record* structure is composed of two basic components: a Data Index and the Data. The format and size of the Data Index is fixed. It describes the contents of Data in the *Record.* The Data

component of each *Record* contains a varying number of *Groups* as indicated by the Data Index. The format and length of data varies from one *Group* to the next; however, all data *Elements* within a single *Group* are of the same type and length. The number of characters in a given *Group* can easily exceed the 120 characters per line limit. In this case, the output overflows to succeeding lines, thus a data *Group* may extend over several Lines.

Each *Group* is given a particular format for its data *Elements*.

11.2.1 Data Index

The Data Index contains a list of 80 three-digit integers. The position in the list corresponds to the data *Group* number. The Group numbers are shown in Table 1. The first integer is the number of elements in the data Group 1, Geophysical Constants; the second integer represents the number of elements in the second data Group, System Description; etc. A value of zero indicates that there is no data for the Group in the Record. Position 80 of the Data Index array has a special meaning. It is used as an SAO format version indicator and is always set to 2 for SAO version 4.0.

11.2.2 Group 1: Geophysical Constants

The values of the Geophysical Constants shown in Table 2 are specified for the station producing the data in the file. Frequencies are in MHz, angles are in degrees.

11.2.3 Group 2: System Description

This Group allows the user to specify the URSI station number or the UMASS Lowell station code and give a description of the system which recorded the data, version numbers of programs used to process the data, etc. An example of the UMLCAR System Description Line is "DPS-4 042/MHJ45, ARTIST 0790, NH 1.3, ADEP 2.19 | " where, for DPS systems, the vertical bar, |, is used to separate the system description from the ADEP operator's message.

11.2.4 Group 3: Ionogram Sounding Settings

This field is intended to allow users to assign codes that identify how the measurement is made with reference to particular sounders. The format of this Group for Digisonde Portable Sounder (DPS) is shown in Table 3. For each particular sounder system, the format of the System Preface Parameters Group must be personalized and a unique Version Indicator should be chosen to distinguish it from other sounder systems. The Version Indicator must consist of two letters; "FF" indicator is used to represent DPS data.

11.2.5 Group 4: Scaled Ionospheric Parameters

The Scaled Ionospheric Parameters are the output of the ARTIST ionogram scaling program. All numbers represent either frequency in Megahertz or altitude in kilometers except the dimensionless MUF factor. The content of each number is explained in Table 4. A frequency value of 999.9 MHz or a height value of 9999 km indicates that no datum is available for this parameter in this ionogram Record. There are currently 47 Scaled Ionospheric Parameters defined.

11.2.6 Group 5: ARTIST Analysis Flags

The ARTIST Analysis Flags are a sequence of two digit integers (60I2 format) which indicate and qualify some of the ARTIST scaled results. Table 5 is a description of the flags and the meaning of their possible values.

11.2.7 Group 6: Doppler Transition Table

The Doppler Translation Table is a sequence of floating point numbers in the 16F7.3 format, which convert the trace Doppler Number into a Doppler frequency in Hertz. These numbers should be read into a floating-point array. Using the Doppler Number as an index to that array will result in the Doppler shift for the scaled trace point in question. The first element of the Doppler translation table corresponds to the Doppler number 0.

11.2.8 ARTIST Trace Points

The ARTIST autoscaled traces are included in this section. The information format and content is identical for any of the F2, F1, E, Es or Ea traces with either Ordinary or eXtraordinary polarization although not all traces may be present in any one ionogram. Currently, the ARTIST program does not scale the complete X-traces, however space has been provided for implementation of this feature at a later date.

The data for each trace are contained in five Groups. For the F2 O-trace they are in Groups 7, 8, 9, 10, and 11; for the F1 O-trace they are in Groups 12, 13, 14, 15, and 16; etc. (see Table 2). There is a one-to-one positional correspondence between elements in these five Groups, in that the first Virtual Height, True Height, Amplitude, Doppler Number and Frequency all correspond to the first Trace point on the ionogram. The same is true of the second point, and so on throughout the entire trace. When trace points are missing they are

represented by a 999. For the virtual height, 0 amplitude and Doppler number.

11.2.9 Groups 7, 12, 17, 22, 26, 30, 43, 47: ARTIST Trace Virtual Heights

This group consists of a number of Virtual Heights for the layer indicated. The number of these heights depends upon the length of the trace on the corresponding ionogram. Virtual Heights are reported in kilometers of altitude.

11.2.10 Groups 8, 13, 18: ARTIST True Heights

This group consists of a number of True Heights for the layer indicated. The number of these heights depends upon the length of the trace on the corresponding ionogram. True Heights are reported in kilometers of altitude. ARTIST4 does not fill these positions and instead uses groups 52-53 for the complete profile listing.

11.2.11 Groups 9, 14, 19, 23, 27, 31, 44, 48: ARTIST Trace Amplitudes

The amplitude in dB of each echo point is recorded.

11.2.12 Groups 10, 15, 20, 24, 28, 32, 45, 49: ARTIST Trace Doppler Numbers

The Doppler Number, as measured by the Digisonde, for each trace point is recorded in 120I1 format. To convert this number to an actual Doppler shift in Hertz, use this integer as the index to the Doppler Translation Table provided in Group 6.

11.2.13 Groups 11, 16, 21, 25, 29, 33, 46, 50: ARTIST Trace Frequencies

The frequency (in MHz) of the trace point is given in this Group. This Group is provided for the possibility of uneven frequency stepping and will normally be empty for ionograms with a constant frequency step. If this group is empty, the frequency of a trace point can be found using the following formula

$$fN = f1 + (N-1) * Df$$

where N is the index of the point in the trace array, ranging from 1 to Ntotal; f1 is the frequency of the first trace point; Df is the frequency step. Df can be obtained from the Ionogram Sounding Settings (Group 3). If character #47 of the DPS preface string (see Table 3) is greater than 1, and character #46 is 0, Df is equal to the Fine Frequency Step, characters #42-45. In all other cases, Df is equal to the Coarse Frequency Step, characters #33-36. The frequency f1 for each ionospheric layer can be obtained using Group 4 (Scaled Ionospheric Parameters) information and Df.

E layer starting frequency is equal to fmin, datum #5 in Table 4.

Es layer starting frequency is equal to fminEs, datum #36 in Table 4.

F1 layer starting frequency is equal to fminF, datum #7 in the Table 4.

If there is no F1 layer detected, the F2 layer starting frequency is equal to fminF, datum #7 in the Table 4. Otherwise, it is equal to foF2 - Df * (NF2 - 1), where NF2 is total number of F2 trace points.

11.2.14 Group 34: Median Amplitude of F Echo

These values are the amplitudes in dB for the F trace. It is calculated every integer MHz between fminF and foF2. The Median Amplitude is calculated by taking the median of the echo amplitudes over a 0.5 MHz interval and normalizing to an altitude of 100 km.

11.2.15 Group 35: Median Amplitude of E Echo

Same as per Code 34, but for the E echo between fminE and foE.

11.2.16 Group 36: Median Amplitude of Es Echo

Same as per Code 34, but for the Es echo between fminE and foEs.

11.2.17 Group 37: True Height Coefficients for the F2 Layer

The True Height Data for F2 layer from the UMLCAR method are stored. There are up to 10 elements. The meaning of each element is given in Table 6.

11.2.18 Group 38: True Height Coefficients for the F1 Layer

The True Height Data for the F1 layer from the UMLCAR method have the same format as those for the F2 layer (Group 37) above, but no zhalfNm value is given (see Table 6).

11.2.19 Group 39: True Height Coefficients for the E Layer

The True Height Data for the E layer from the UMLCAR method have a format very similar to that for the F2 and F1 layers (Codes 37 and 38) above, except there are only seven elements stored in this Group. The first four parameters are fstart, fend, zpeak and dev as defined for the F2 layer.

There are, however, only three coefficients for the shifted Chebyshev polynomials (A0 - A2) for the E layer true height.

11.2.20 Group 40: Valley Parameters

This Group was used in pervious releases of SAO format for parameters describing the valley region, and is no longer used. Group 42 replaces Group 40 in the new SAO format.

11.2.21 Group 41: Edit Flags

The edit flags are written in 120I1 format indicating whether the data are edited with ADEP (flag=1), whether the data are not edited (flag=0), i.e. the autoscaled value is used, or whether they are from long term prediction (flag=2). The position in the edit flag list corresponds to the order of the characteristics listed in Table 4 with some additions. A complete list is given in Table 7. The edit flags are used to set the slash (/) indicators in the URSI-IIWG Characteristics database.

11.2.22 Group 42: Valley Parameters for UMLCAR model

The current content for this Group is two parameters describing the width and depth of the valley region in the UMLCAR valley model.

References

Gamache R. R. and B. W. Reinisch, "Ionogram Characteristics at Uneven Data Rates," Presented at URSI Working Group G.4 Ionospheric Informatics International Workshop, July, 1989., University of Lowell Center for Atmospheric Research, 1989a.

Gamache R. R., I.A. Galkin, and B. W. Reinisch, "A Database Record Structure for Ionogram Data", University of Lowell Center for Atmospheric Research, UMLCAR 96-01, 1996.

Huang X. and B.W.Reinisch, Vertical .Electron density profiles from the Digisonde network, Adv. Space Res. **6**, 121-129, 1996

Reinisch, B.W., D.M. Haines,.K. Bibl, I. Galkin, X. Huang, D.F. Kitrosser, G.S. Sales, and J.L. Scali, Ionospheric sounding in support of over-the-horizon radar, Radio Sci. **32**, 4,1681-1694, 1997b.

Reinisch, B. W. and X. Huang, Fitting the IRI F2-profile function to measured bottomside profiles, Adv. Space Res., in print, 1997

Table 1. SAO Record Format

Group	Format	Description
	2(40I3	DATA FILE INDEX
1	16F7.3	GEOPHYSICAL CONSTANTS
2	fm3	SYSTEM DESCRIPTION: Version numbers, etc.
3	fm4	IONOGRAM SOUNDING SETTINGS (PREFACE)
4	fm5	SCALED IONOSPHERIC PARAMETERS
5	fm6	ANALYSIS FLAGS
6	fm2	DOPPLER TRANSLATION TABLE
		O-TRACE POINTS - F2 LAYER
7	fm1	VIRTUAL HEIGHTS
8	fm1	TRUE HEIGHTS
9	fm10	AMPLITUDES
10	fm7	DOPPLER NUMBERS
11	fm8	FREQUENCIES
		O-TRACE POINTS - F1 LAYER
12	fm1	VIRTUAL HEIGHTS
13	fm1	TRUE HEIGHTS
14	fm10	AMPLITUDES
15	fm7	DOPPLER NUMBERS
16	fm8	FREQUENCIES
		O-TRACE POINTS - E LAYER
17	fm1	VIRTUAL HEIGHTS
18	fm1	TRUE HEIGHTS
19	fm10	AMPLITUDES
20	fm7	DOPPLER NUMBERS
21	fm8	FREQUENCIES
		X-TRACE POINTS - F2 LAYER
22	fm1	VIRTUAL HEIGHTS
23	fm10	AMPLITUDES
24	fm7	DOPPLER NUMBERS
25	fm8	FREQUENCIES

Table 1. SAO Record Format (Continued)

Group	Format	Description
		X-TRACE POINTS - F1 LAYER
26	fm1	VIRTUAL HEIGHTS
27	fm10	AMPLITUDES
28	fm7	DOPPLER NUMBERS
29	fm8	FREQUENCIES
		X-TRACE POINTS - E LAYER
30	fm1	VIRTUAL HEIGHTS
31	fm10	AMPLITUDES
32	fm7	DOPPLER NUMBERS
33	fm8	FREQUENCIES
34	fm10	MEDIAN AMPLITUDES OF F ECHOES
35	fm10	MEDIAN AMPLITUDES OF E ECHOES
36	fm10	MEDIAN AMPLITUDES OF ES ECHOES
37	fm9	TRUE HEIGHTS F2 LAYER DATA UMLCAR METHOD
38	fm9	TRUE HEIGHTS F1 LAYER DATA UMLCAR METHOD
39	fm9	TRUE HEIGHTS E LAYER DATA UMLCAR METHOD
40	fm9	VALLEY DESCRIPTION POLW,POLD,W,V
41	fm7	EDIT FLAGS
42	fm9	W,D of UMLCAR VALLEY DESCRIPTION
		O-TRACE POINTS - Es LAYER
43	fm1	VIRTUAL HEIGHTS
44	fm6	AMPLITUDES
45	fm7	DOPPLER NUMBERS
46	fm8	FREQUENCIES
		O-TRACE POINTS - AURORAL E LAYER
47	fm1	VIRTUAL HEIGHTS
48	fm6	AMPLITUDES
49	fm7	DOPPLER NUMBERS
50	fm8	FREQUENCIES

Table 2. Geophysical Constants

Position	Description
1	Gyrofrequency (MHz)
2	Dip angle (-90.0 to 90.0 degrees)
3	Geographic Latitude (-90.0 to +90.0 degrees)
4	Geographic Longitude East(0.0 to 359.9 degrees)
5	Sunspot Number for the current year

Table 3. System Preface Parameters

Number	Description	Possible Values
1-2.	Preface Version Indicator	AA,AB, .. ZZ
3-6.	4 digit Year.	(1976)
7-9.	Day of Year	(1-366)
10-11.	Month	(1-12)
12-13.	Day of Month	(1-31)
14-15.	Hour [All times and dates correspond to UT.]	(0-23)
16-17.	Minutes	(0-59)
18-19.	Seconds	(0-59)
20-22.	Receiver Station ID (three digits)	042
23-25.	Transmitter Station ID.	042
26.	DPS Schedule	(1-6)
27.	DPS Program	(1-7)
28-32.	Start Frequency, 1 kHz resolution	(01000 - 45000)
33-36.	Coarse Frequency Step, 1 kHz resolution	(1-2000)
37-41.	Stop Frequency, 1 kHz resolution	(01000 - 45000)
42-45.	DPS Fine Frequency Step, 1 kHz resolution	(0000 - 9999)
46.	Multiplexing disabled [0 - multiplexing enabled, 1 - disabled].	(0,1)
47.	Number of DPS Small Steps in a scan	(1 to F)
48.	DPS Phase Code	(1-4, 9-C)
49.	Alternative antenna setup [0 - standard, 1 - alternative].	(0,1)
50.	DPS Antenna Options	(0 to F)
51.	Total FFT samples [power of 2]	(3-7)
52.	DPS Radio Silent Mode [1 - no transmission]	(0,1)
53-55.	Pulse Repetition Rate (pps)	(0-999)
56-59.	Range Start, 1 km resolution	(0-9999)
60.	DPS Range Increment [2 - 2.5 km, 5 - 5 km, A - 10 km]	(2,5,A)
61-64.	Number of ranges	(1-9999)
65-68.	Scan Delay, 15 km units	(0-1500)
69.	DPS Base Gain	(0-F, encoded)
70.	DPS Frequency Search Enabled	(0,1)
71.	DPS Operating Mode [0 - Vertical beam, 5 - multi-beam ionogram]	(0-7)
72.	ARTIST Enabled	(0,1)
73.	DPS Data Format [1 - MMM, 4 - RSF, 5 - SBF]	(0-6)
74.	On-line printer selection [0 - no printer,1 - b/w, 2 - color]	(0,1,2)
75-76.	Ionogram thresholded for FTP transfer [0-no thresholding]	(0-20, encoded)
77.	High interference condition [1 - extra 12 dB attenuation]	(0,1)

Table 4. ARTIST Scaled Characteristics

#	Description	Units	Range	Accuracy	Precision
1	foF2 : F2 layer critical frequency, including the adjustment by the true height profile algorithm	MHz	within the ionogram frequency range	at least quarter of frequency increment	1 kHz
2	foF1 : F1 layer critical frequency	MHz	within the ionogram frequency range	1 frequency increment	1 kHz
3	M(D) = MUF(D)/foF2	-	variable	-	-
4	MUF(D) : Maximum usable frequency for ground distance D	MHz	variable	1 frequency increment	1 kHz
5	fmin: minimum frequency of ionogram echoes	MHz	within the ionogram frequency range	1 frequency increment	1 kHz
6	foEs : Es layer critical frequency	MHz	within the ionogram frequency range	1 frequency increment	1 kHz
7	fminF : Minimum frequency of F-layer echoes	MHz	within the ionogram frequency range	1 frequency increment	1 kHz
8	fminE : Minimum frequency of E-layer echoes	MHz	within the ionogram frequency range	1 frequency increment	1 kHz
9	foE : E layer critical frequency	MHz	within the ionogram frequency range	1 frequency increment	1 kHz
10	fxI : Maximum frequency of F-trace	MHz	within the ionogram frequency range	1 frequency increment	1 kHz
11	h'F : Minimum virtual height of F trace	km	within the ionogram height range	1 height increment	1 m
12	h'F2 : Minimum virtual height of F2 trace	km	within the ionogram height range	1 height increment	1 m
13	h'E : Minimum virtual height of E trace	km	within the ionogram height range	1 height increment	1 m
14	h'Es : Minimum virtual height of Es trace	km	within the ionogram height range	1 height increment	1 m
15	zmE : Peak height of E-layer	km	variable	1 height increment	1 m
16	yE : Half thickness of E layer	km	variable	1 height increment	1 m
17	QF : Average range spread of F layer	km	variable	1 height increment	1 m
18	QE : Average range spread of E layer	km	variable	1 height increment	1 m
19	DownF : Lowering of F trace to the leading edge	km	0-pulse width	1 height increment	1 m
20	DownE : Lowering of E trace to the leading edge	km	0-pulse width	1 height increment	1 m
21	DownEs : Lowering of Es trace to the leading edge	km	0-pulse width	1 height increment	1 m
22	FF : Frequency spread between fxF2 and fxI	MHz	variable	1 frequency increment	1 kHz

Table 4. ARTIST Scaled Characteristics (Continued)

#	Description	Units	Range	Accuracy	Precision
23	FE : Frequency spread beyond foE	MHz	variable	1 frequency increment	1 kHz
24	D : Distance for MUF calculation	km	within the ionogram height range	1 km	1 m
25	fMUF : MUF/OblFactor	MHz	within the ionogram frequency range	1 frequency increment	1 kHz
26	h'(fMUF) : Virtual height at MUF/OblFactor frequency	MHz	within the ionogram height range	1 height increment	1 m
27	delta_foF2 : Adjustment to the scaled foF2 during profile inversion	MHz	less than a frequency increment	1 kHz	1 kHz
28	foEp : predicted value of foE	MHz	variable	±0.3 MHz	1 kHz
29	f(h'F) : frequency at which h'F occurs	MHz	within the ionogram frequency range	1 frequency increment	1 kHz
30	f(h'F2) : frequency at which h'F2 occurs	MHz	within the ionogram frequency range	1 frequency increment	1 kHz
31	foF1p : predicted value of foF1	MHz	variable	± 0.5 MHz	1 kHz
32	peak height of F2 layer	km	variable		1 m
33	peak height of F1 layer	km	variable		1 m
34	zhalfNm : the true height at half the maximum density in the F2 layer	km	variable	1 km	1 m
35	foF2p : predicted value of foF2	MHz	variable	± 2.0 MHz	1 kHz
36	fminEs : minimum frequency of Es layer	MHz	within the ionogram frequency range	1 frequency increment	1 kHz
37	yF2 : half thickness of the F2 layer, parabolic model	km	variable	100 m	1 m
38	yF1 : half thickness of the F1 layer, parabolic model	km	variable	100 m	1 m
39	TEC : total electron content	1016 m-2		-	-
40	Scale height at the F2 peak	km	variable	1km	1km
41	B0, IRI thickness parameter	km	typically 70-110	-	-
42	B1, IRI profile shape parameter	-	0.1-6.0	-	-
43	foEa, critical frequency of auroral E layer	MHz	variable	1 frequency increment	1 kHz
44	h'Ea, minimum virtual height of auroral E layer trace	km	variable	1 height increment	1 m
45	foP, highest ordinary wave critical frequency of F region patch trace	MHz	variable	1 frequency increment	1 kHz
46	h'P, minimum virtual height of the trace used to determine foP	km	variable	1 height increment	1 m

Table 5. ARTIST Analysis Flags

Position	Content	Description
1	1	E-region from scaled data
	2	E-region predicted
2	N	True height inversion error codes
3	N	Number of roots found in plasma scale height function of the F profile
4	0	foF1 not scaled
	1	foF1 scaled
5	0	No AWS Qualifier applies
	1	Blanketing Sporadic E
	2	Non-Deviative Absorption
	3	Equipment Outage
	4	foF2 greater than equipment limits
	5	fmin lower than equipment limits
	6	Spread F
	7	foF2 less than foF1
	8	Interference
	9	Deviative absorption
7	N	Number of roots found in plasma scale height function of the E profile
8	N	Number of roots found in plasma scale height function of the F1 profile
10	0-5	Confidence level, 0-highest confidence, 5-lowest confidence
9,11-19		Not used
20		Internal ARTIST use

Table 6. True Height Coefficients for F2 Layer

Position	Parameter	Description
1	fstart	Start frequency (MHz) of the F2 layer
2	fend	The end frequency of the F2 layer
3	zpeak	The height of the peak of the F2 layer
4	dev	The average fitting error in km/point.
5-9	A0-A4	Shifted-Chebyshev polynomial coefficients
10	zhalfNm	Height at half peak electron density

Table 7. ADEP Edit Flags

#	Scaled Characteristic	Description
1	foF2	F2 layer critical frequency calculated by hyperbolic fit
2	foF1	F1 layer critical frequency
3	M(D)	M-factor, MUF(D)/foF2, for distance D
4	MUF(D)	Maximum usable frequency for distance D
5	fmin	Minimum frequency for E or F echoes
6	foEs	Es layer critical frequency
7	fminF	Minimum frequency of F-trace
8	fminE	Minimum frequency of E-trace
9	foE	E layer critical frequency
10	fxI	Maximum frequency of F-trace
11	h'F	Minimum virtual height of F trace
12	h'F2	Minimum virtual height of F2 trace
13	h'E	Minimum virtual height of E trace
14	h'Es	Minimum virtual height of Es layer
15	HOM	Peak of E layer using parabolic model
16	Ym	Corresponding half thickness of E layer
17	QF	Average range spread of F-trace
18	QE	Average range spread of E-trace
19	Down F2	Lowering of F-trace maximum to leading edge
20	Down E	Lowering of E-trace maximum to leading edge
21	Down Es	Lowering of Es-trace maximum to leading edge
22	FF	Frequency spread between fxF2 and fxI
23	FE	As FF but considered beyond foE
24	D	Distance used for MUF calculation
25	fMUF(D)	MUF(D)/obliquity factor[2]
26	h'MUF(D)	Virtual height at fMUF
27	foF2c	correction to add to foF2 to get actual foF2
28	foEp	Predicted foE
29	f(h'F)	Frequency at which hminF occurs
30	f(h'F2)	Frequency at which hminF2 occurs

bliquity factor(h', D) is the ratio of frequencies for vertical and oblique propagation to distance D with virtual height h'.

Table 7. ADEP Edit Flags (Continued)

#	Scaled Characteristic	Description
31	foF1p	Predicted foF1
32	Zpeak	Peak height F2 layer
33	ZpeakF1	Peak height F2 layer
34	zhalfnm	Height at half peak electron density
35	foF2p	Predicted foF2
36	fminEs	Minimum frequency of Es layer
37	YF2	Half-thickness of F2 layer in parabolic model
38	YF1	Half-thickness of F1 layer in parabolic model
39	TEC	Total electron content
40	HscaleF2	Scale height at F2 peak
41	B0	IRI thickness parameter
42	B1	IRI profile shape parameter
43	foEa	Critical frequency of auroral E layer
44	h'Ea	Minimum virtual height of auroral E layer trace
45	foP	Highest ordinary wave critical frequency of F region patch trace
46	h'P	Minimum virtual height of the trace used to determine foP
50	F2 trace	F2 trace points were edited
51	F1 trace	F1 trace points were edited
52	E trace	E trace points were edited
53	z(h)	true height was recalculated with edited traces
54	Es trace	Es trace points were edited

International Geophysical Calendar 1998 (Final)

(See other side for information on use of this calendar)

	S	M	T	W	T	F	S
JANUARY					1	2	3
	4	5	6	7	8	9	10
	11	12	(13)	14	(15)	16	17
	18	19	20+	21+	22	23	24
	25	26	27*	28N*	29	30	31
FEBRUARY	1	2	3	4	5	6	7
	8	9	10	11	12	13	14
	15	16	(17)	18	(19)	20	21
	22	23	24	25*	26N*	27	28
MARCH	1	2	3	4	5	6	7
	8	9	10	11	12	13	14
	15	16	(17)	18	(19)	20	21
	22	23+	24+	25+	26+	27+	28N
APRIL	29	30	31	1	2	3	4
	5	6	7	8	9	10	11
	12	13	14	15	16	17	18
	19	20	(21)	22*	(23)*	24	25
	26N	27+	28+	29+	30	1	2
MAY	3	4	5	6	7	8	9
	10	11	12	13	14	15	16
	17	18	(19)	20*	(21)*	22	23
	24	25N	26+	27+	28+	29	30
JUNE	31	1	2	3	4	5	6
	7	8	9	10	11	12	13
	14	15	(16)	17	(18)	19	20
	21	22	23*+	24N*+	25	26	27
	28	29	30				
	S	M	T	W	T	F	S

	S	M	T	W	T	F	S
JULY				1	2	3	4
	5	6	7	8	9	10	11
	12	13	(14)	15	(16)	17	18
	19	20	21	22*	23N*	24	25
AUGUST	26	27	28	29	30	31	1
	2	3	4	5	6	7	8
	9	10	11	12	13	14	15
	16	17	(18)+	(19)*+	(20)*	21	22N
SEPTEMBER	23	24	25	26	27	28	29
	30	31	1	2	3	4	5
	6	7	8	9	10	11	12
	13	14	15	16	17	18	19
OCTOBER	20N	21+	(22)*+	(23)*+	(24)+	25+	26
	27	28	29	30	1	2	3
	4	5	6	7	8	9	10
	11	12	13	14	15	16	17
NOVEMBER	18	19+	(20)N+	(21)*+	(22)*	23	24
	25	26	27	28	29	30	31
	1	2	3	4	5	6	7
	8	9	10	11	12	13	14
DECEMBER	15	16+	(17)+	(18)*+	(19)N*+	20	21
	22	23	24	25	26	27	28
	29	30	1	2	3	4	5
	6	7	8+	9+	10	11	12
1999 JANUARY	13	14	(15)	(16)*+	(17)*	18N	19
	20	21	22	23	24	25	26
	27	28	29	30	31	1	2
	3	4	5	6	7	8	9
	10	11	(12)	(13)*	(14)*	15	16N
	17	18	19	20	21	22	23
	24	25	26	27	28	29	30
	31						
	S	M	T	W	T	F	S

(13) Regular World Day (RWD)

(18) Priority Regular World Day (PRWD)

14 Quarterly World Day (QWD) also a PRWD and RWD

7 Regular Geophysical Day (RGD)

12 13 World Geophysical Interval (WGI)

6 + Incoherent Scatter Coordinated Observation Day

N New Moon

26 Day of Solar Eclipse

22 23 Airglow and Aurora Period

27* Dark Moon Geophysical Day (DMGD)

NOTES on other dates and programs of interest:

1. Days with **significant meteor shower** activity are: Northern Hemisphere 3-5 Jan; 21-23 Apr; 4-6 May; 6-11, 27-29 Jun; 11-14 Aug; 21-23 Oct; 16-19 Nov; 13-15, 22-24 Dec 1998; 3-5 Jan 1999. Southern Hemisphere 4-6 May; 6-11, 27-29 Jun; 27 Jul-2 Aug; 21-23 Oct; 16-19 Nov; 13-15 Dec 1998. These can be studied for their own geophysical effects or may be "geophysical noise" to other experiments. Particular attention is drawn to the Leonid shower which is expected to produce storm conditions of thousands to tens of thousands of visual meteors per hour at approximately 17 UT +/- 4 h on Nov 17, 1998.

2. **GAW (Global Atmosphere Watch)** -- early warning system for changes in greenhouse gases, ozone layer, and long range transport of pollutants. (See Explanations.)

3. **ISCS (International Solar Cycle Studies)** -- SCOSTEP Project. Observing Program 1998-2002: Study of processes associated with the rising and maximum phase of the solar cycle. (See Explanations.)

4. **+ Incoherent Scatter Coordinated Observations Days** (see Explanations) starting at 1600 UT on the first day of the intervals indicated, and ending at 1600 UT on the last day of the intervals: 20-21 Jan DATABASE; 23-27 Mar MLTCS/CADITS; 27-29 Apr WLS; 26-28 May POLITE; 23-24 Jun DATABASE; 18-19 Aug DATABASE; 21-25 Sep MLTCS/CADITS; 19-21 Oct WLS; 16-19 Nov POLITE; 8-9 Dec DATABASE